3. Imaging system of x-ray microscopy

Optical layout

Principles of zone plate

Phase contrast

Tomography

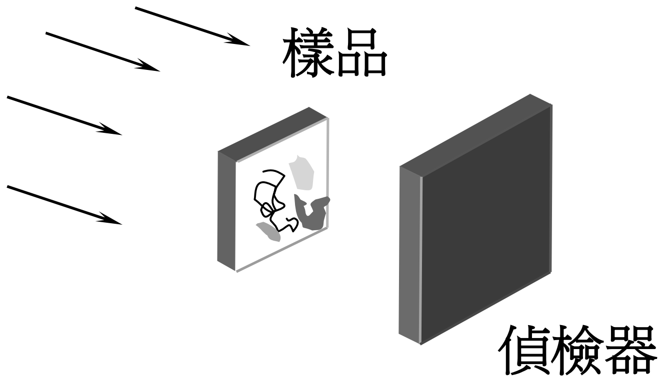

Projection

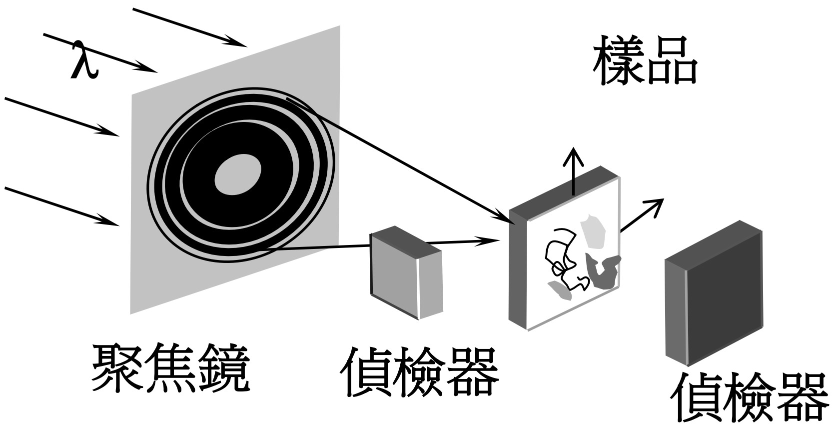

STXM(Scanning Transmission X-ray Microscopy)

TXM(Transmission X-ray Microscopy)

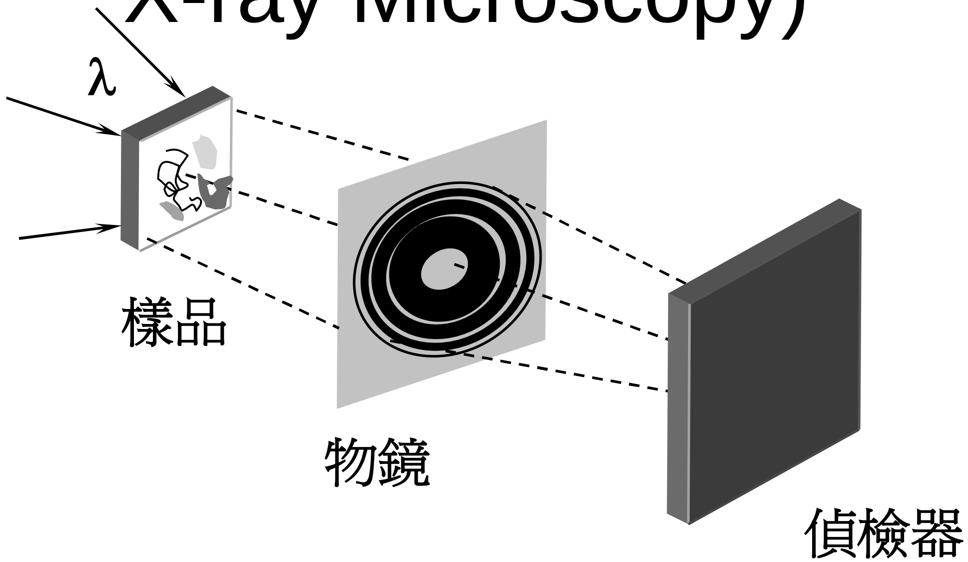

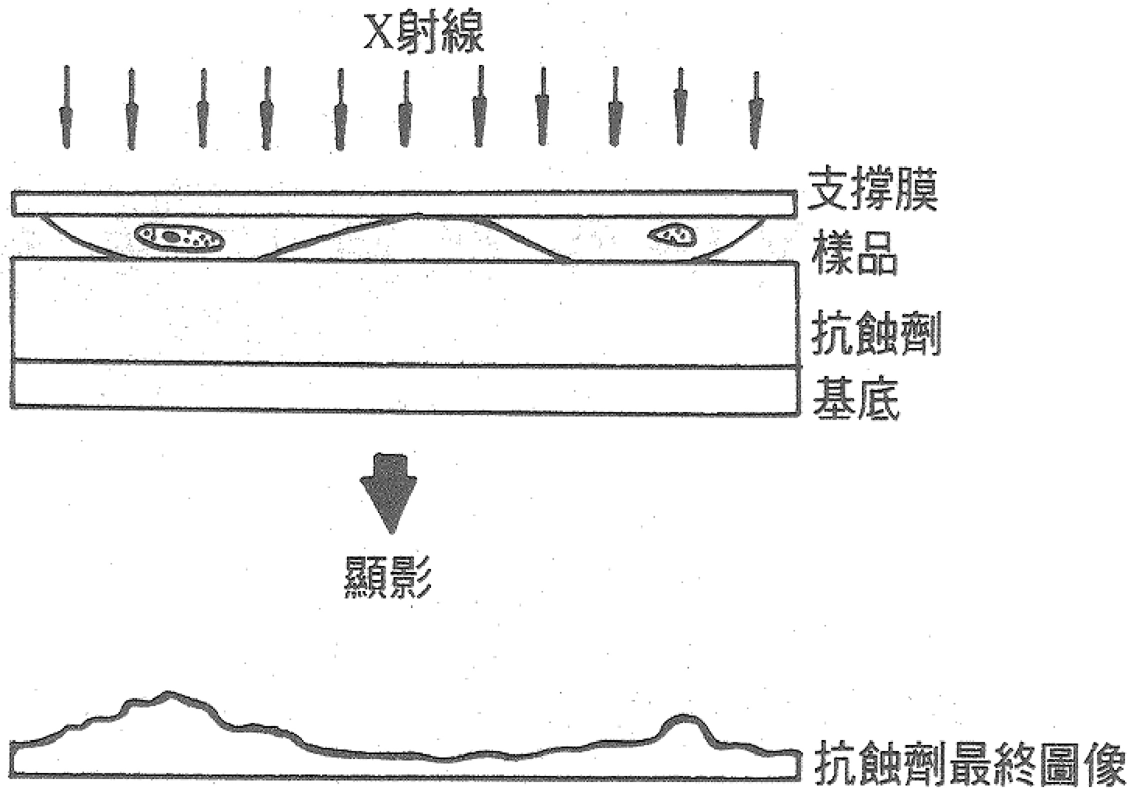

圖 4.1　接觸X射線顯微術原理圖

Optical Layout of NSRRC nano-TXM (I)

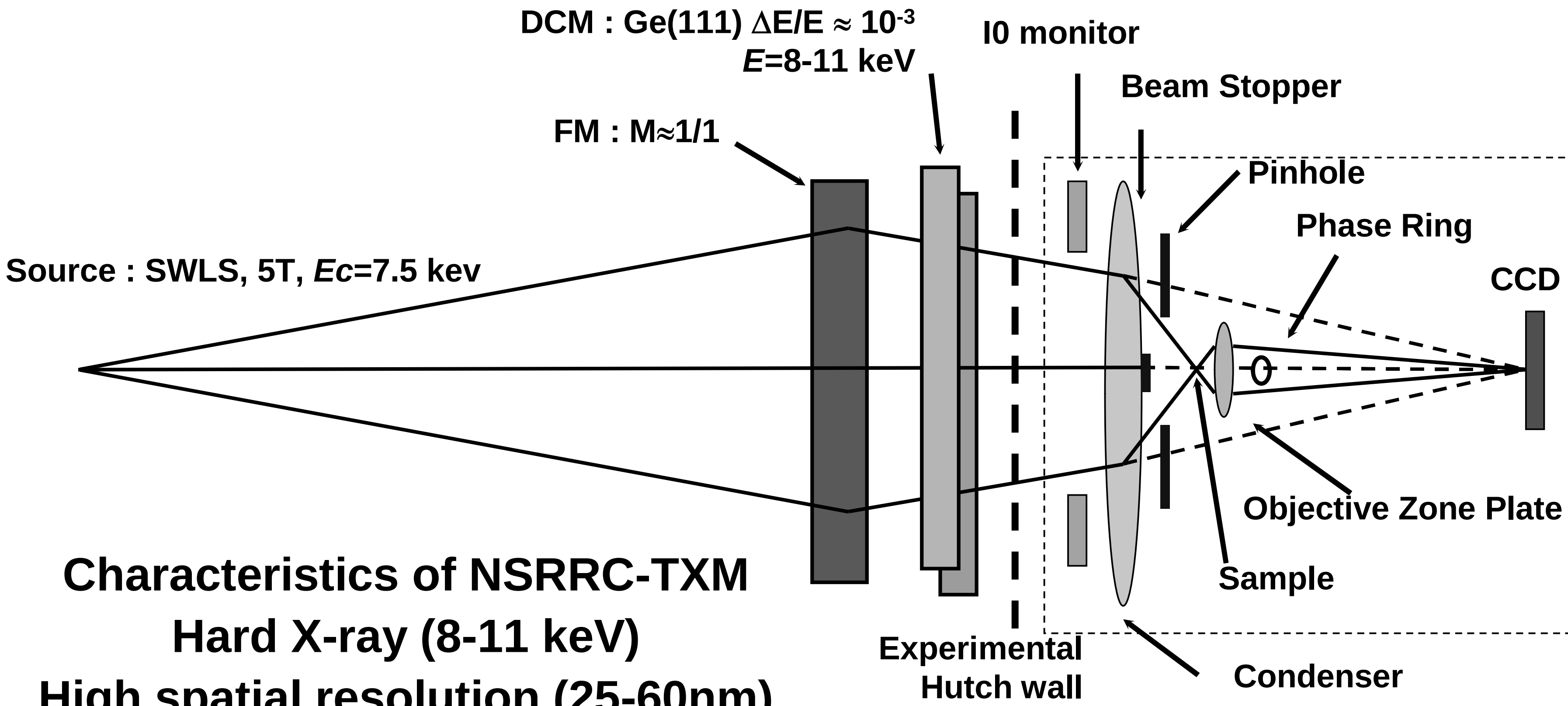

Characteristics of NSRRC-TXM

Hard X-ray (8-11 keV)

High spatial resolution (25-60nm)

Short exposure time

3D tomography

Phase contrast

Optical Layout of NSRRC nano-TXM (II)

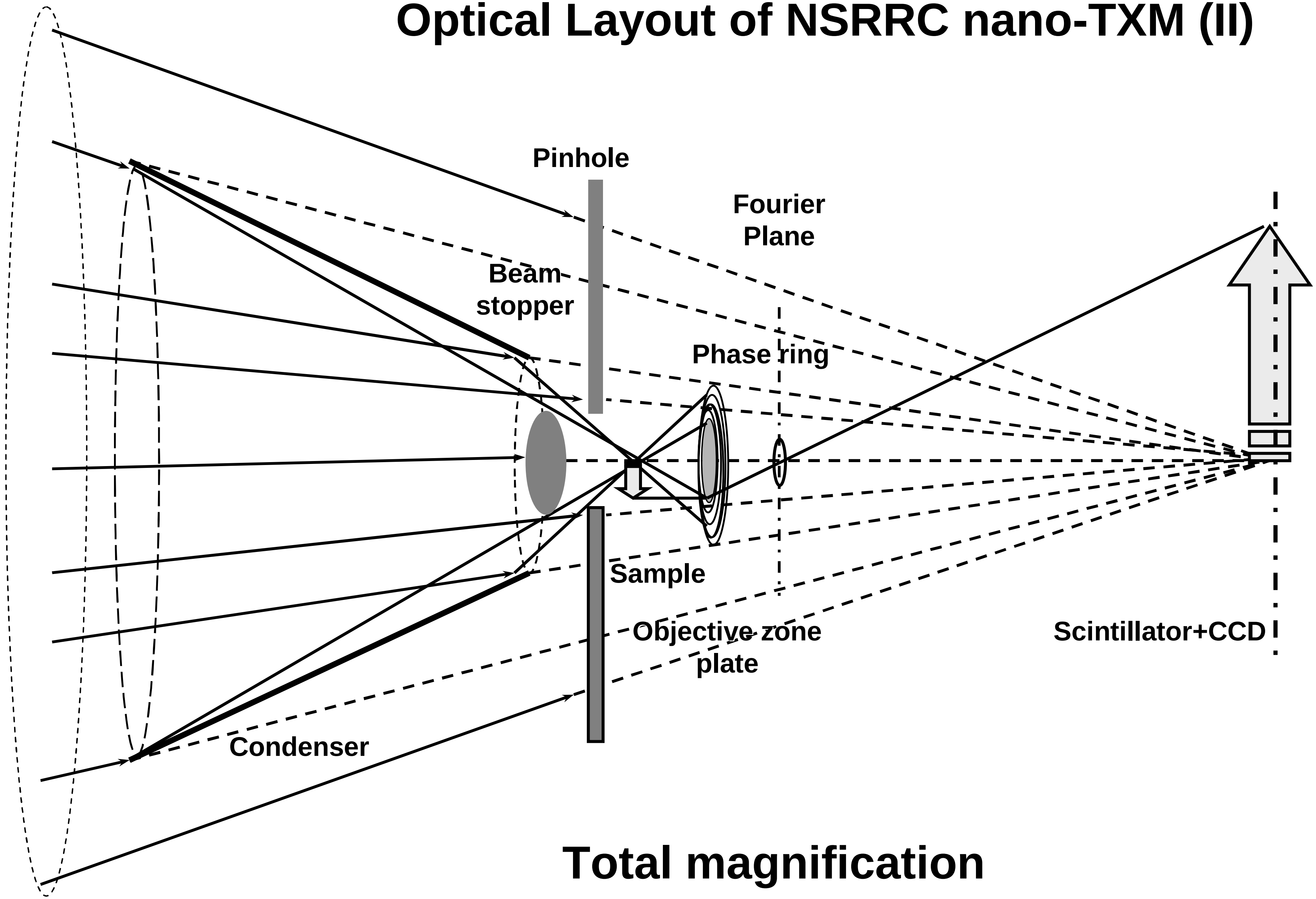

Total magnification
X880 (60nm) and X2640(30nm)

Layout of superconducting wavelength shifter beamlines BL01A, BL01B and BL01C.

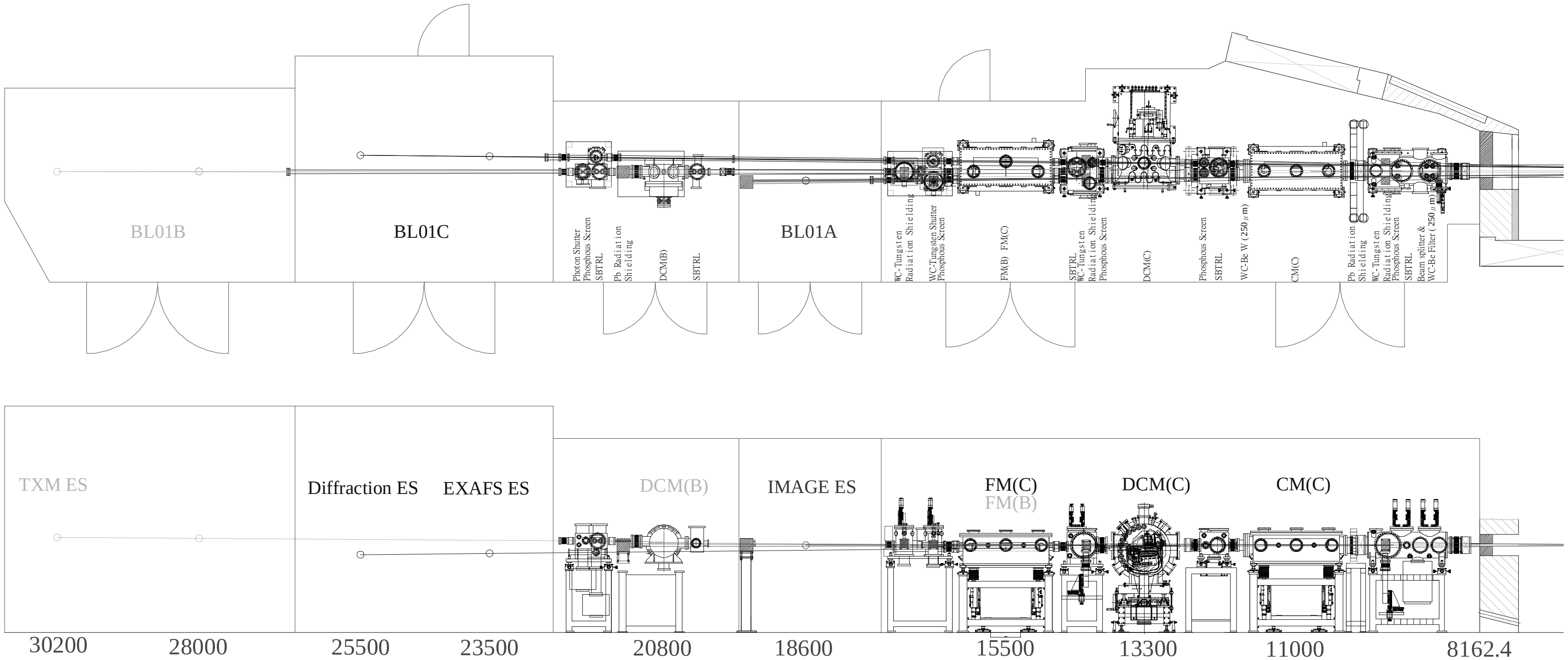

Nano-TXM at BL01B (overview)

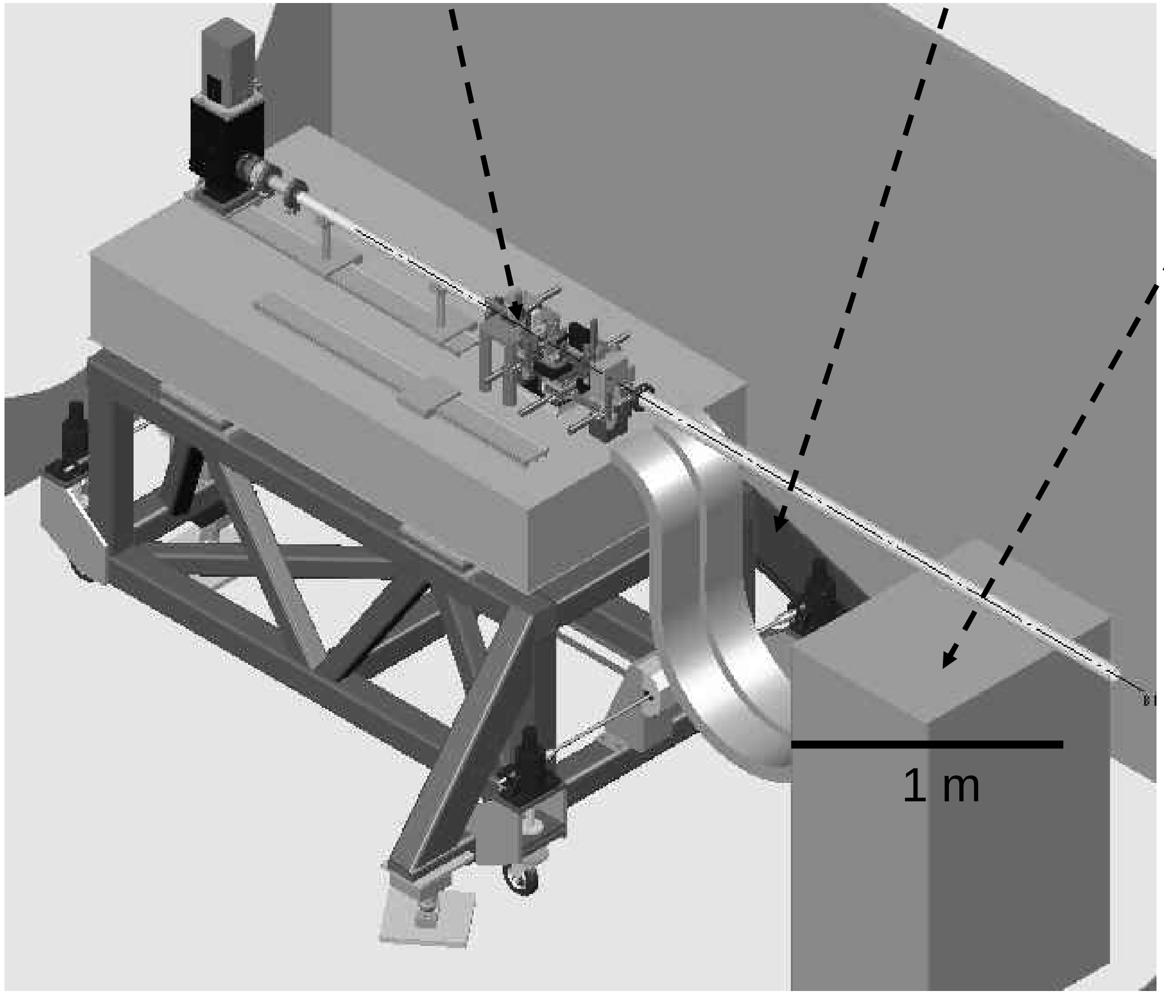

Installation started on September 13, 2004.

Nano-TXM (optical)

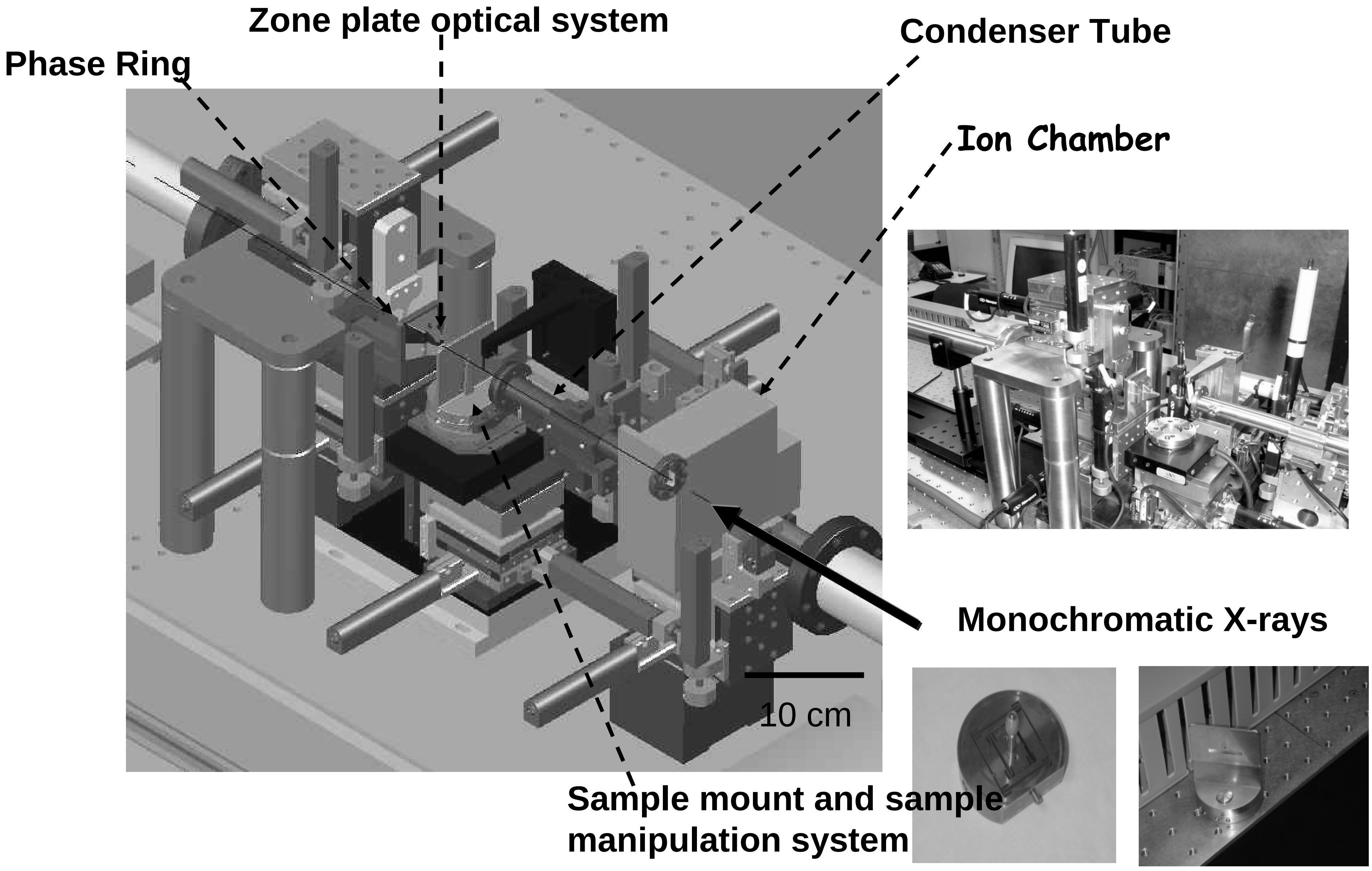

A Fresnel Zone Plate Lens Used as a Diffractive Lens for Point to Point Imaging

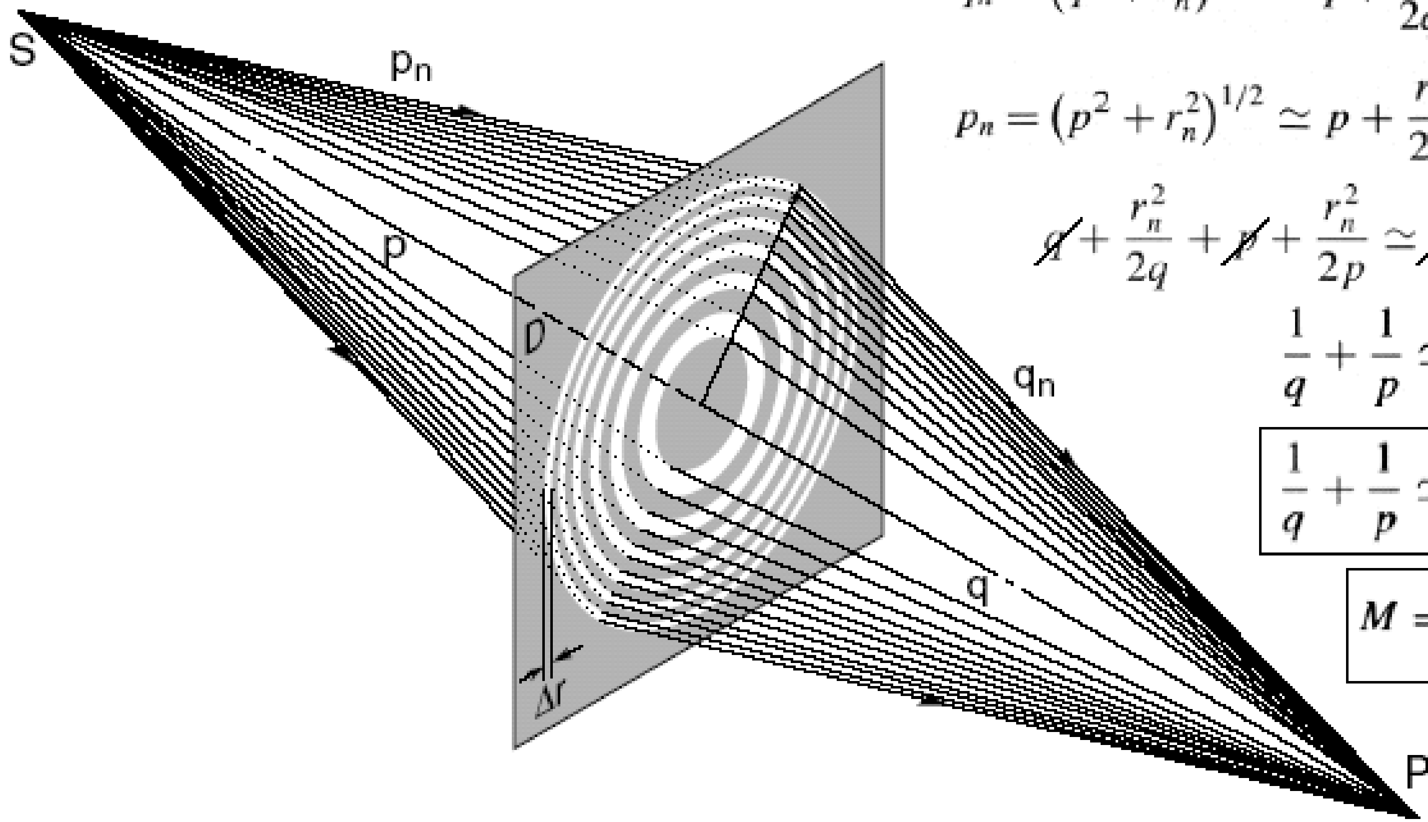

$$q_n + p_n = q + p + \frac{n\lambda}{2}$$

$$q_n = \left(q^2 + r_n^2\right)^{1/2} \simeq q + \frac{r_n^2}{2q}$$

$$p_n = \left(p^2 + r_n^2\right)^{1/2} \simeq p + \frac{r_n^2}{2p}$$

$$\cancel{q} + \frac{r_n^2}{2q} + \cancel{p} + \frac{r_n^2}{2p} \simeq \cancel{q} + \cancel{p} + \frac{n\lambda}{2}$$

$$\frac{1}{q} + \frac{1}{p} \simeq \frac{n\lambda}{r_n^2}$$

$$\boxed{\frac{1}{q} + \frac{1}{p} \simeq \frac{1}{f}} \quad (9.17)$$

$$\boxed{M = \frac{p}{q}} \quad (9.18)$$

Zone Plate Diffractive Focusing for Higher Orders

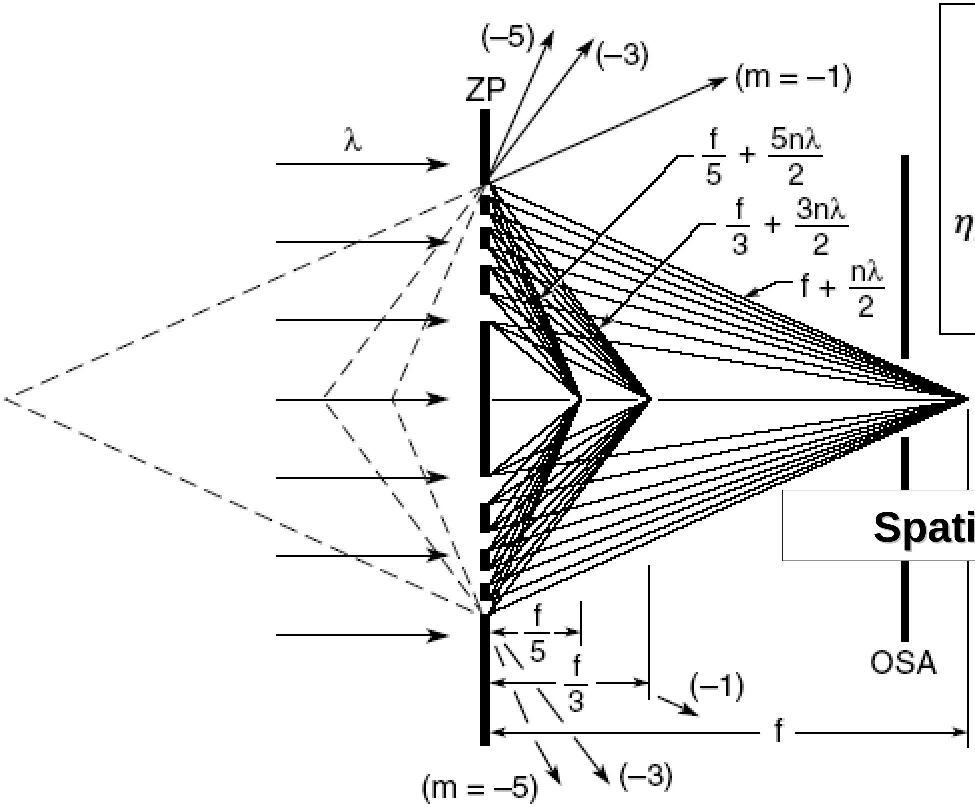

$$r_n^2 \simeq mn\lambda f_m \qquad (9.19)$$

$$\eta_m = \begin{cases} \frac{1}{4} & m = 0 \\ 1/m^2\pi^2 & m \text{ odd} \\ 0 & m \text{ even} \end{cases} \qquad (9.24)$$

Spatial Resolution | **$d_m = 1.22 dr_n / m$**

Courtesy of D. Attwood, Soft X-ray and EUV Radiation

Zone plate consists of concentric rings (zones) with zone width decreasing with radius.

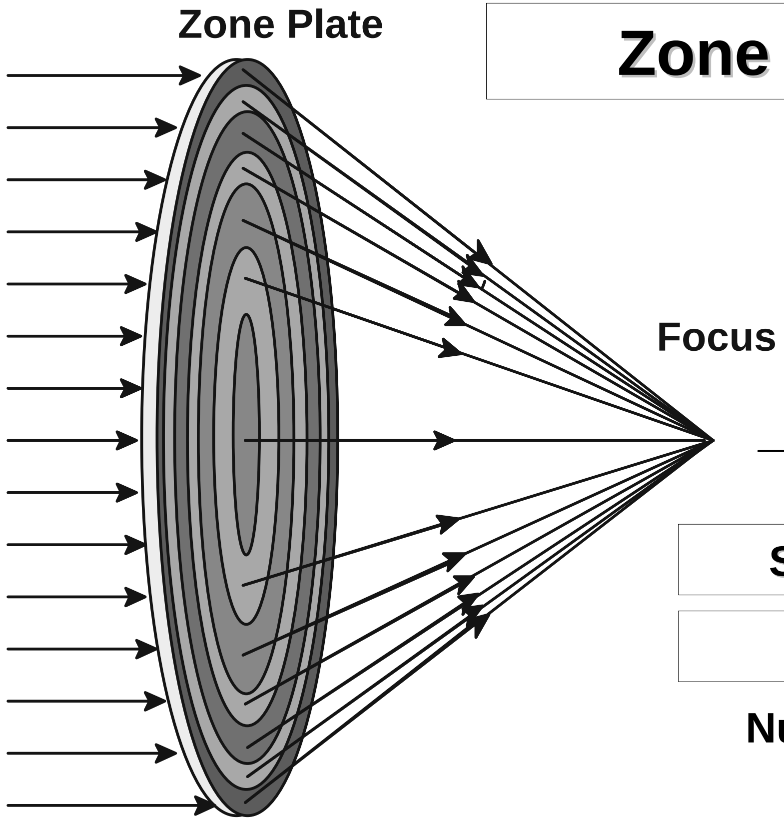

Zone Plate Equations

f : focal length
n : zone index
λ : wavelength
m : diffraction order (1,3,5)
r : radius of the zone plate
dr_n: outermost zone width

Zone Radius	$r_n = (n f \lambda)^{1/2}$
Spatial Resolution	$d_m = 1.22 dr_n / m$
Focal Length	$f_m = 2 r dr / (m \lambda)$
Numerical Aperture	$NA = \lambda / (2 dr)$

When NA <<1, the ZP can be treated like an ordinary refractive lens, i.e., $1/q + 1/p = 1/f$ and $M = q / p$.

Zone Plate's Key Parameters

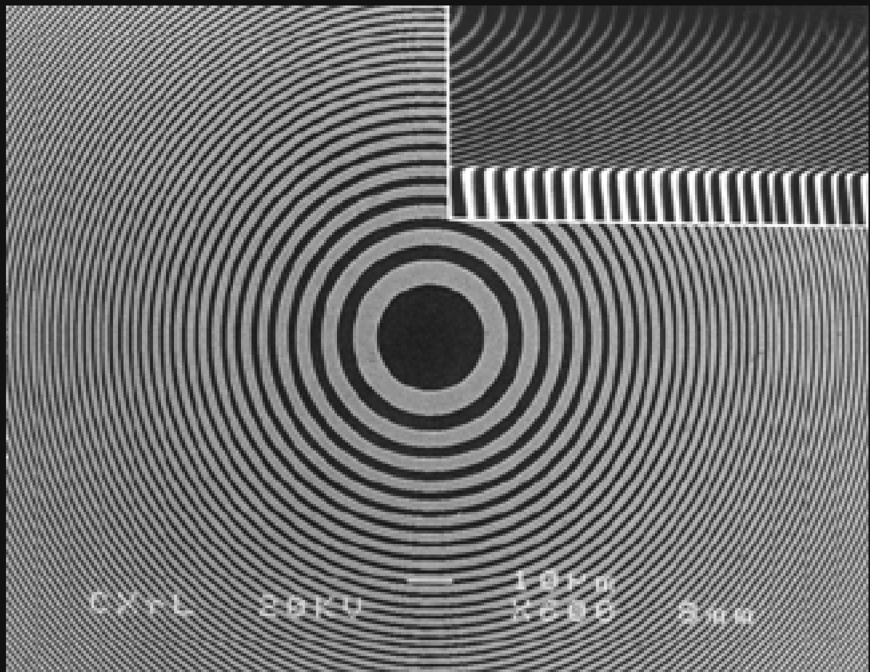

SEM Image of a ZP and its zone profile

Key parameters:

Number of zones

  > 100 required for good focusing

Outermost (smallest) zone width

  Determines resolution and NA

Zone materials, thickness, profile

  Focusing efficiency

Focal length

  Working distance

Zone Plate Performance

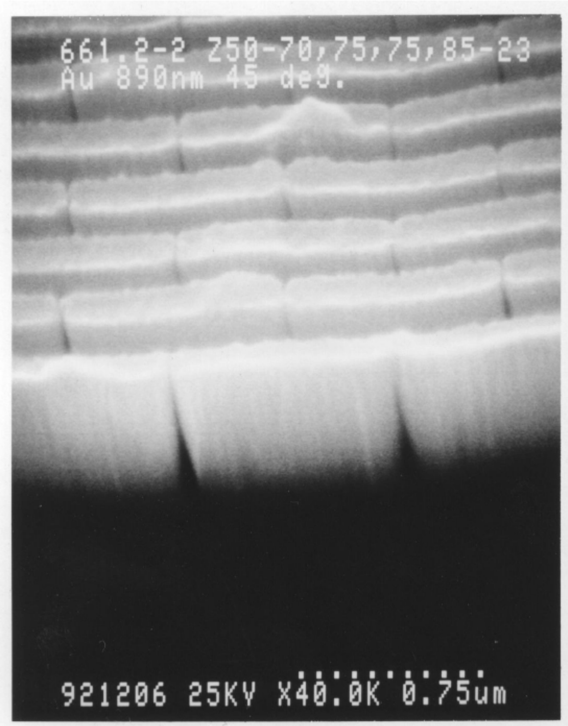

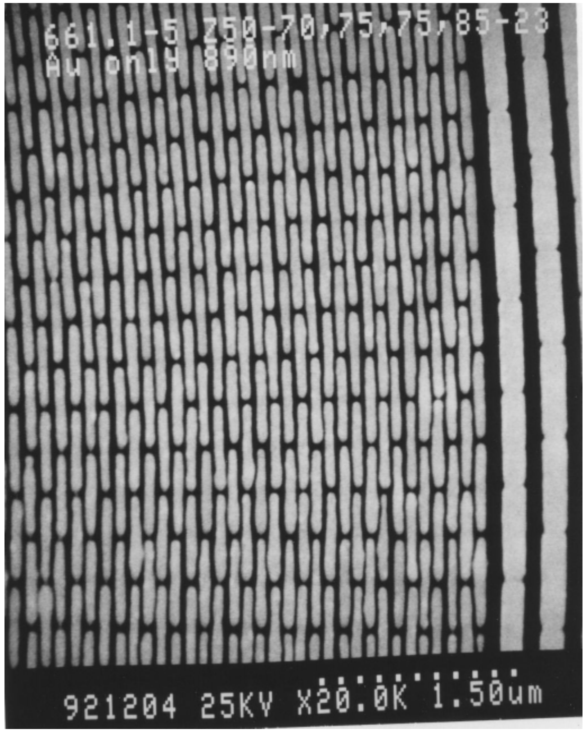

50nm zone width
with 890nm Height

Zone plate
efficiency~=15%

Outermost-zone
AR=17.8

Table 4 Zone Plate Specifications

Outmost zone width:	50 nm
Diameter of the first zone plate lens:	85 μm
Diameter of the second zone plate lens:	75 μm
Diameter of the third zone plate lens:	70 μm
The common focal length at 8.5, 9.5, and 10.5 keV	30 mm
Zone Construction Material:	Au
Aspect ratio:	>15:1
Support membrane:	1 um Si_3N_4 membrane
Focusing efficiency:	> 10%

Using Phase Effects to Achieve Higher Diffraction Efficiency

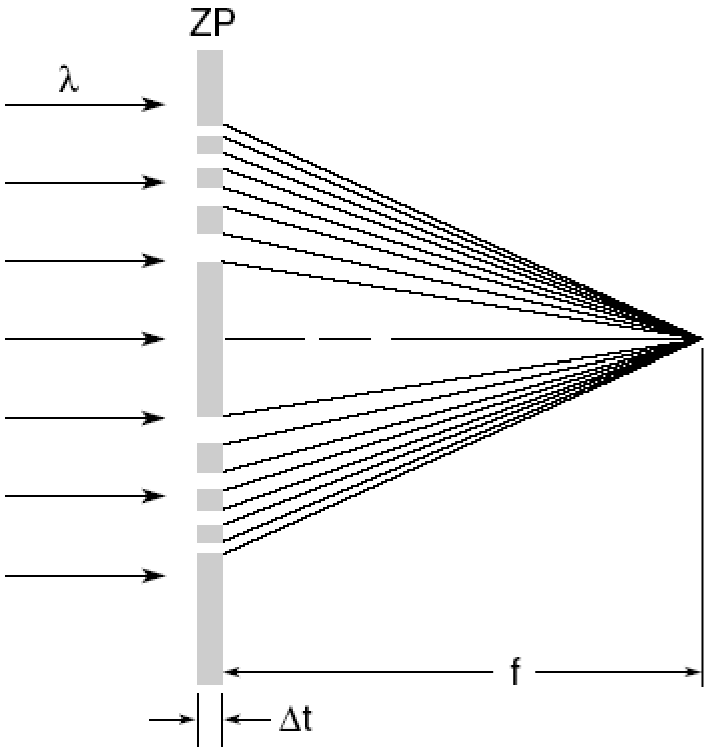

$$\Delta\phi = \left(\frac{2\pi\delta}{\lambda}\right)\Delta t \qquad (3.29)$$

For a π-phase shift

$$\boxed{\Delta t = \frac{\lambda}{2\delta}} \qquad (9.25)$$

a factor of four can be gained in diffraction efficiency. For soft x-rays and EUV all materials are partially absorbing

$$n = 1 - \delta + i\beta \qquad (3.12)$$

Optimization is a function of δ/β, as discussed by J. Kirz, J. Opt. Soc. Am. 64, 301 (1974) and by G.R. Morrison, Ch. 8 in A. Michette and C. Buckley, X-Ray Science and Technology (IOP, Bristol, 1993).

Challenges of Zone Plate Fabrication

Precise high aspect ratio nano-structuring in high mass density materials, e.g. Au

Aspect ratio (AR) required for optimal focusing efficiency of x-rays in an Au zone plate

	Spatial Resolution	
Energy (keV)	**60nm (50nm zone width)**	**30nm (25nm Zone width)**
8.0	**18**	**36**
9.0	**20**	**40**
10.0	**23**	**46**
11.0	**25**	**50**

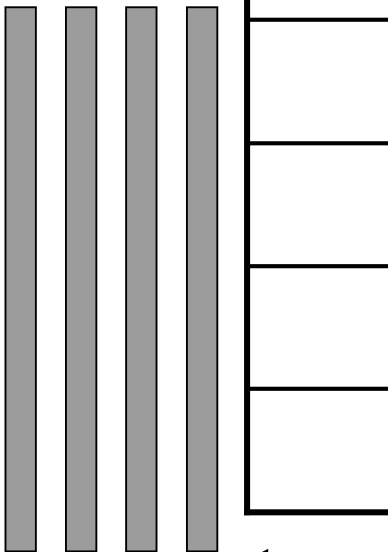

Grating structure with an aspect ratio of 18

Processing of a Gold Zone Plate

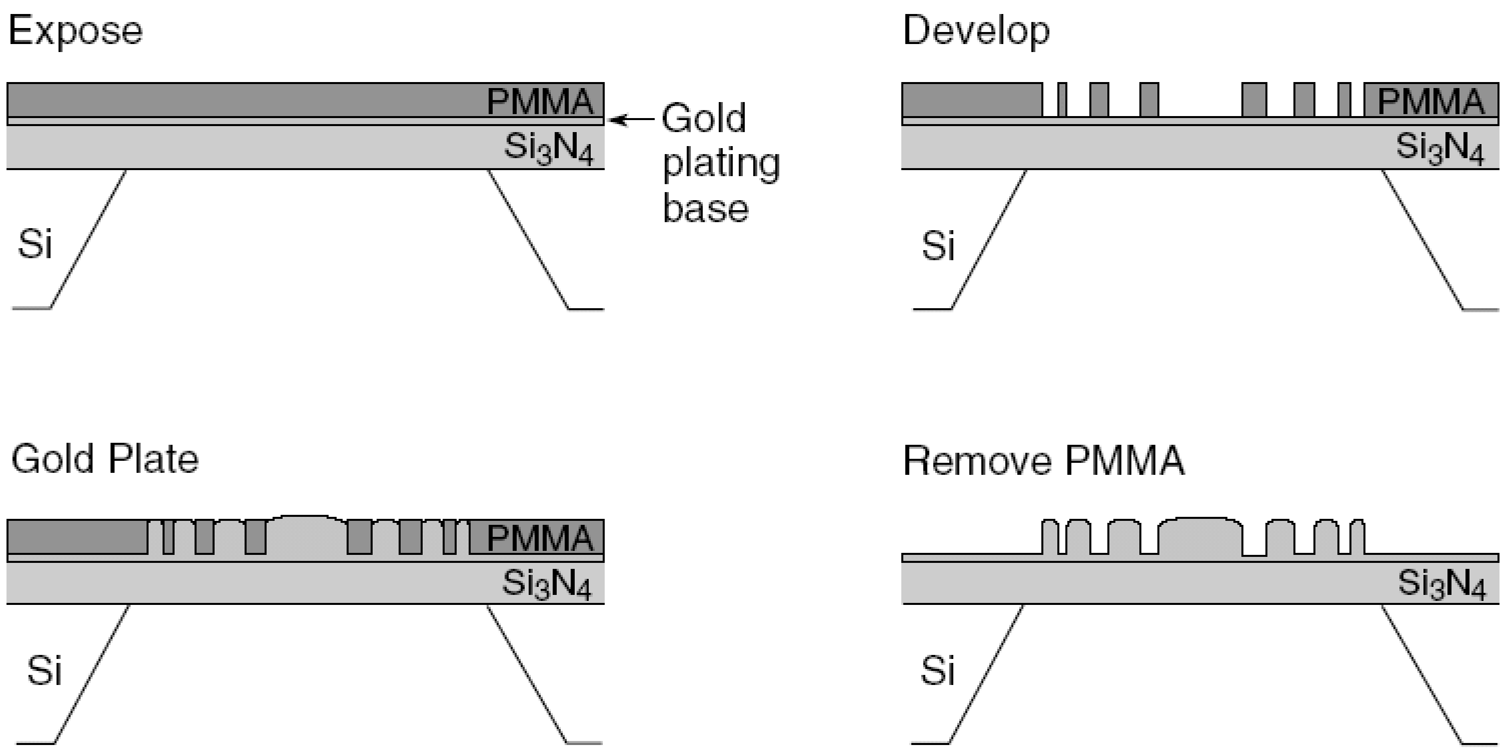

Courtesy of E. Anderson, LBNL

Phase contrast helps

Refraction index : $n = 1-\delta-i\beta$

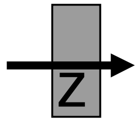

$$E(z)=E_0 e^{-i2\pi(-\delta-i\beta)\, z/\lambda} = E_0 e^{i2\pi\delta z/\lambda\, -2\pi\beta z/\lambda}$$

$$I(z) \sim |E(z)|^2 \sim I_0 e^{4\pi\beta z/\lambda}$$

Absorption contrast

$$\mu z = 4\pi\beta z/\lambda \sim \lambda^3$$

Phase contrast

$$\phi(z) = 2\pi\delta z/\lambda \sim \lambda$$

Zernike's phase contrast method in optical microscopy was invented in 1935 and Zernike was awarded the 1953 Noble Prize in Physic for this great achievement, making the observation of the biology transparent tissue come true. With the same approaches, the low-z material, biology tissue and dielectric material can be imaged by the full field x-ray microscope.

- Phase contrast is x10^4 higher than absorption contrast for protein in water @ 8keV
- Required dose reduced due to phase contrast

Kirz (1995): 0.05μm protein in 10μm thick ice

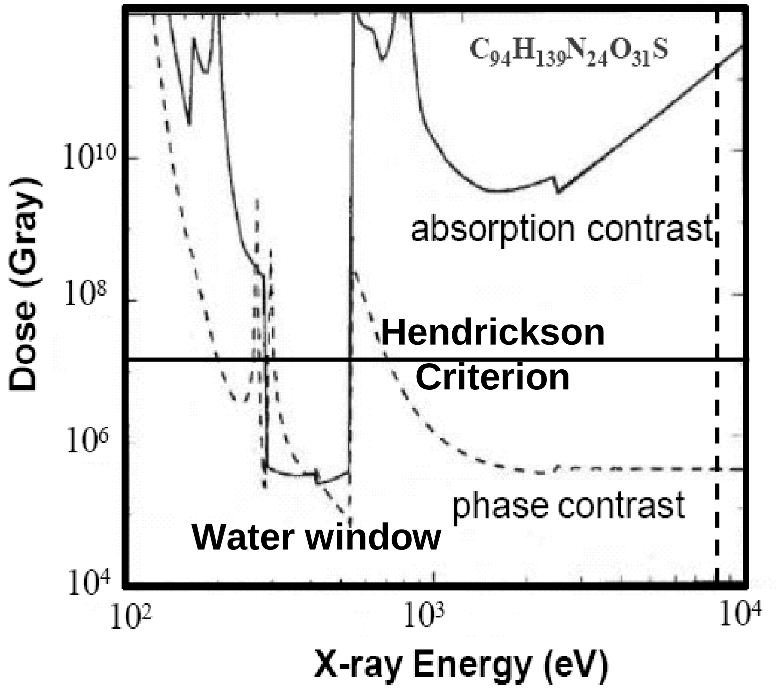

Zernike’s Phase Contrast Method in TXM

G. Schneider (1998)

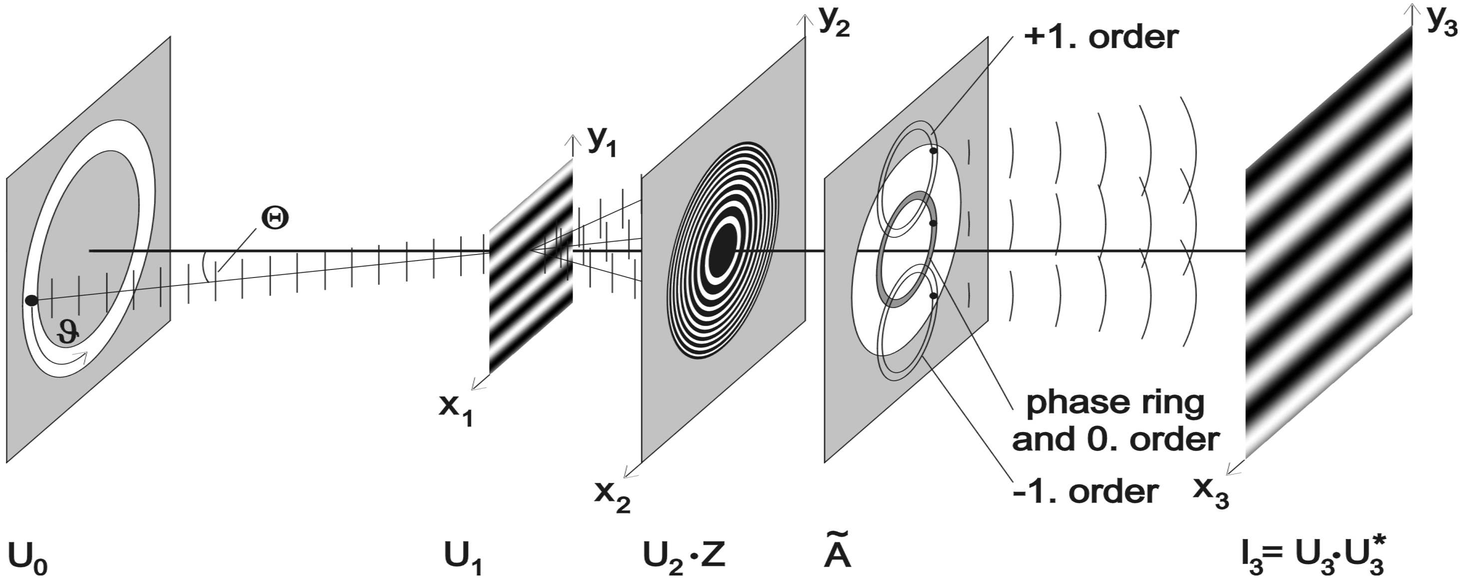

$$g(y) = e^{i\varphi(y)} \sim 1 + i\,\varphi(y)$$

$$\mathcal{F}[G(y)] \sim U_1(\nu) + i\,U_2(\nu)$$

$$\mathcal{F}^{-1}[i\,U_1(\nu) + i\,U_2(\nu)] \sim g_1(y') + g_2(y')$$

Superior Modulation Transfer Function of X-ray Phase Contrast Imaging to Allow Detecting Smaller Defects

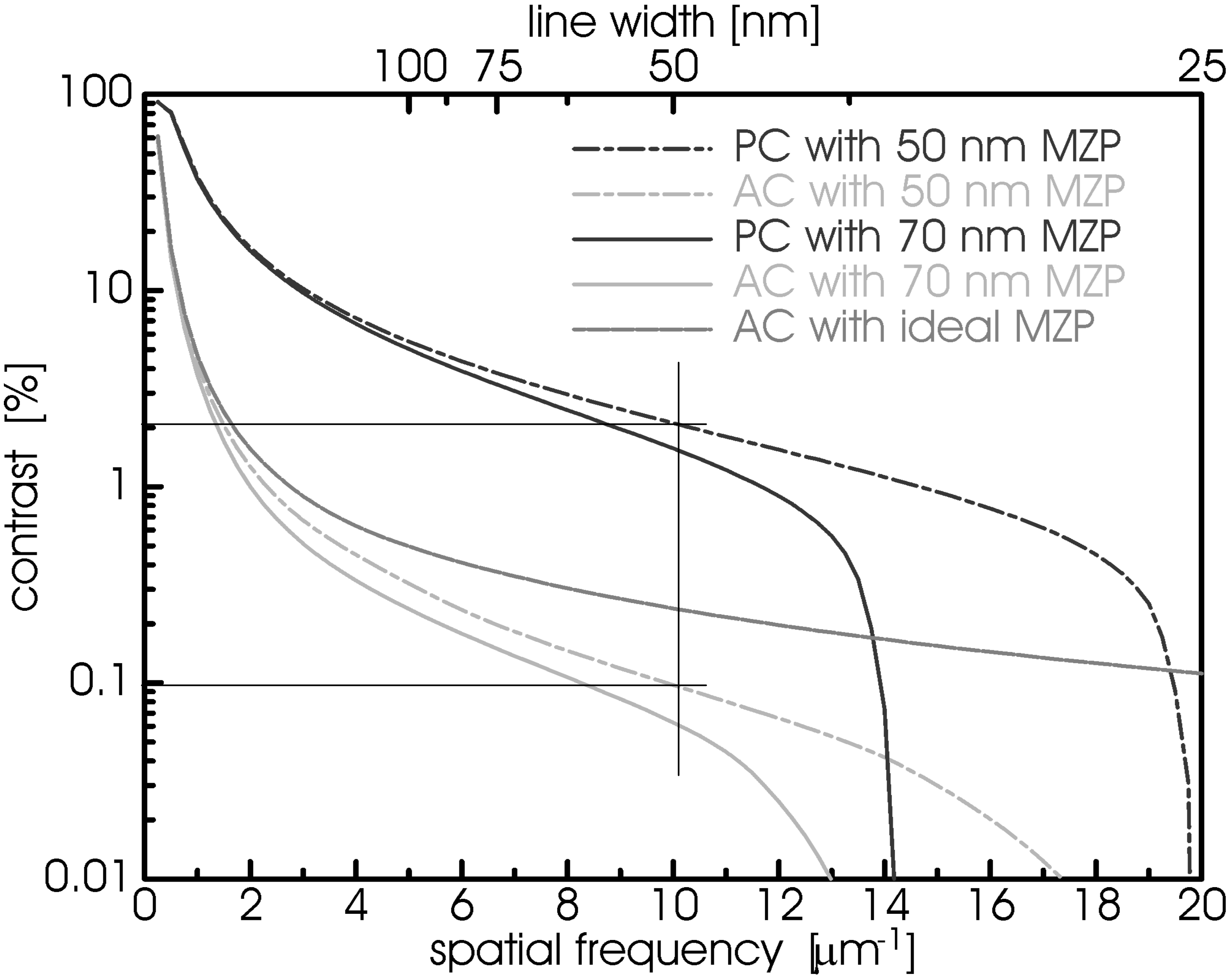

Courtesy of G. Schneider

Phase contrast X-ray microscopy @ 4 keV – Applications I

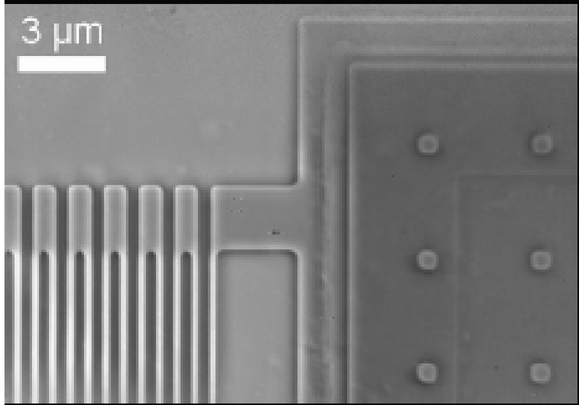

Positive phase contrast 45 %
(0.7 µm high Ni phase ring)

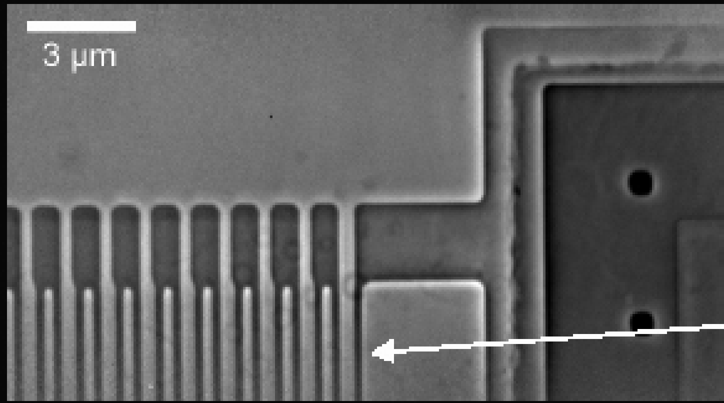

Negative phase contrast 40 %
(2.2 µm high Ni phase ring)

SEMATECH-Sample:
Copper Interconnects within a SiO_2 dielectric in a serpentine resistor, smallest line width 225 nm

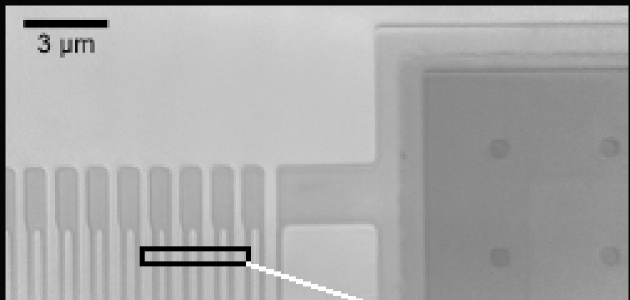

In comparison:
Amplitude contrast 7 %

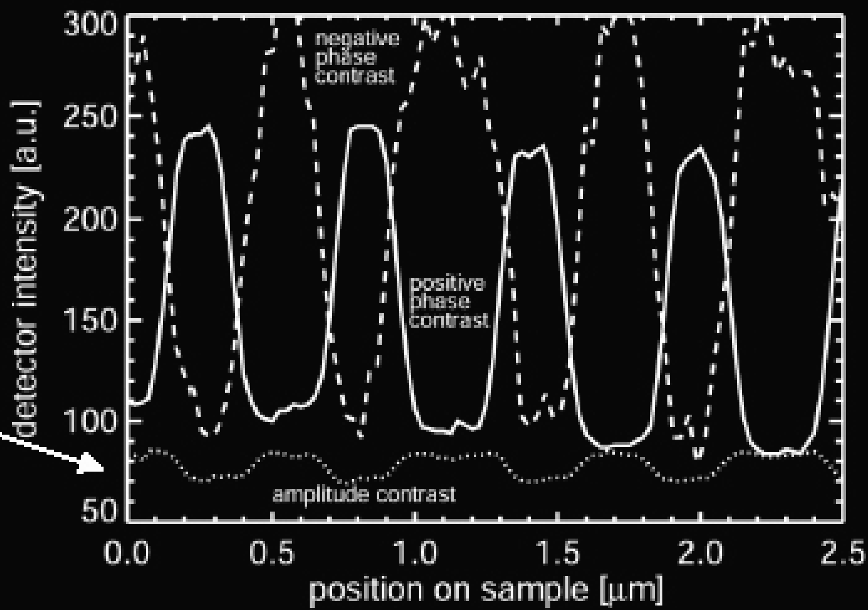

Contrast reversal between:

- Amplitude contrast and positive phase contrast
- positive and negative phase contrast image

Phase Contrast Images of a Plastic Zone Plate

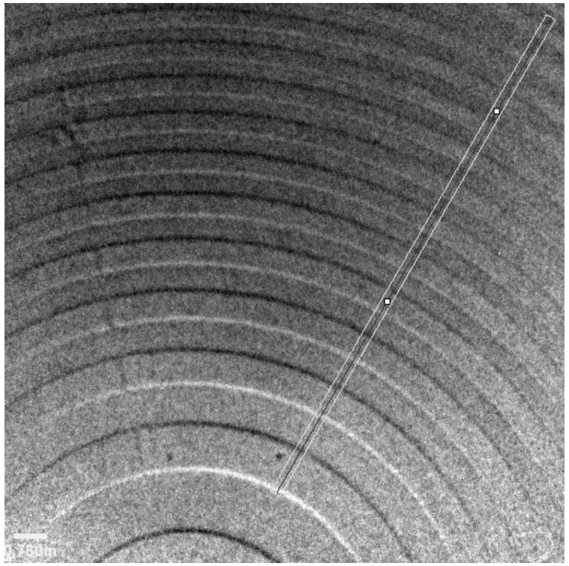

Without phase contrast

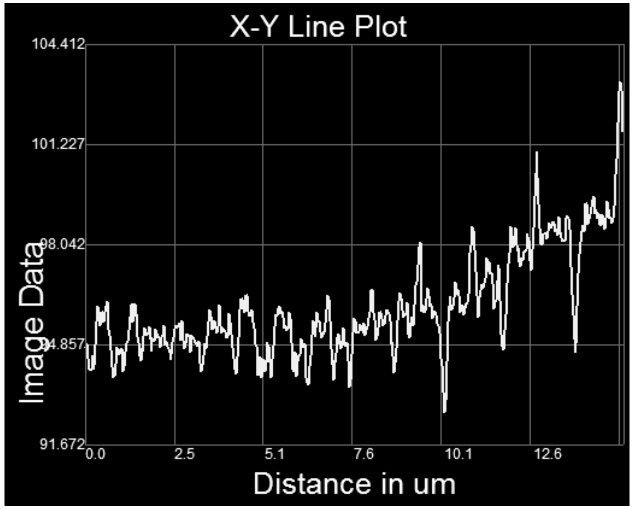

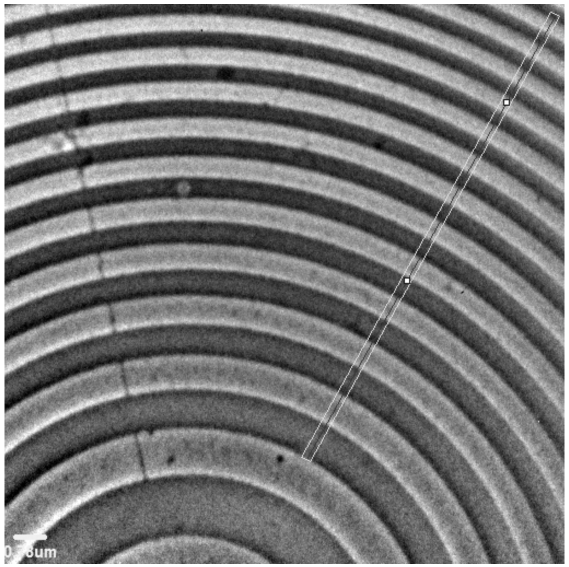

With phase contrast

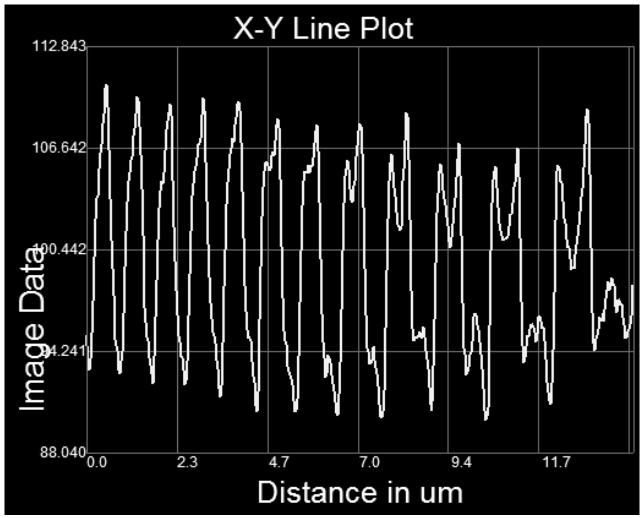

Plastic zone-plate
provided by *Xradia Inc*.

Rock from Gi-Gi Earthquake TXM (1111.29m, well A)

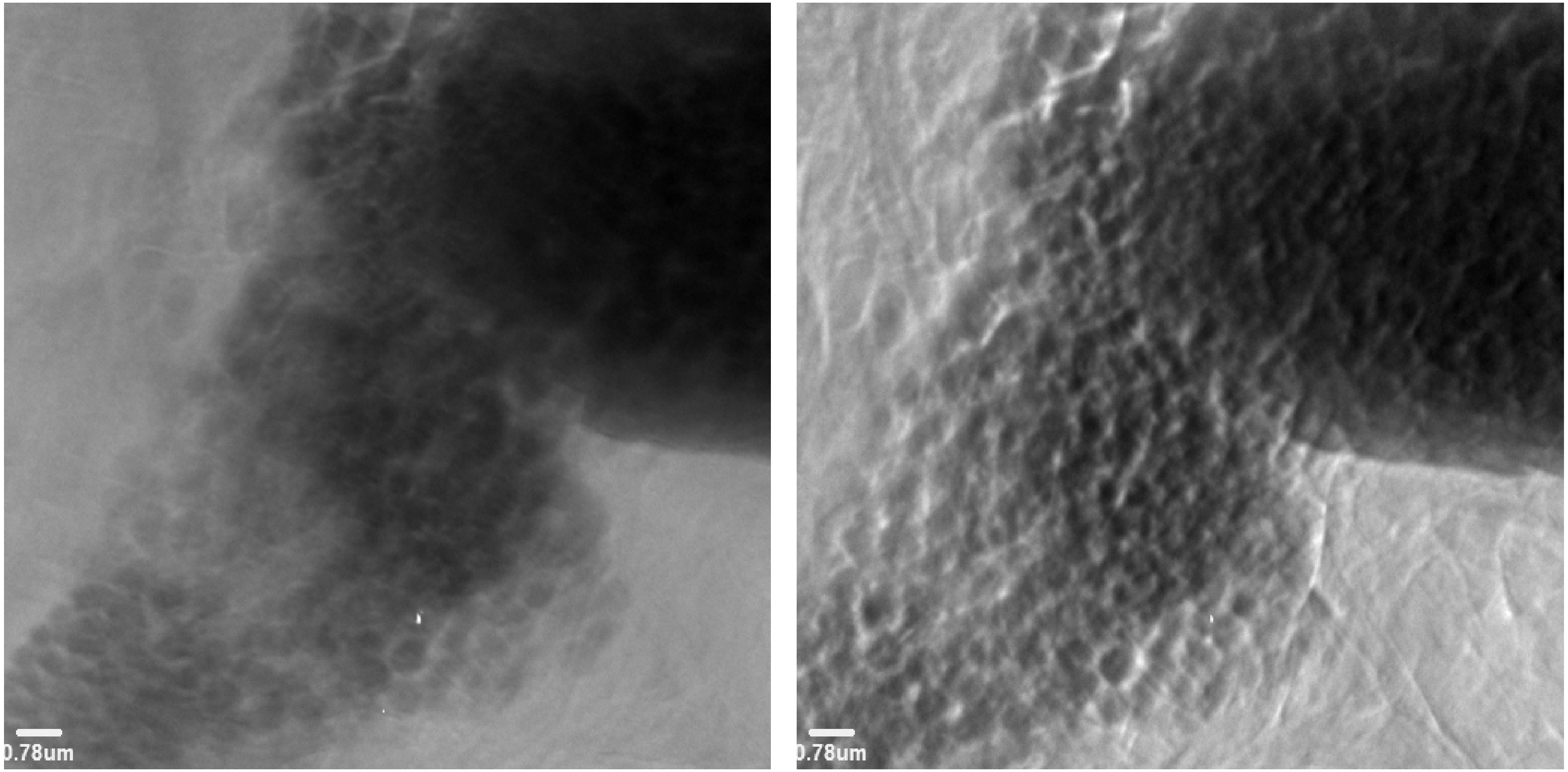

Absorption

Phase contrast

Schematic Representation of the Tomography Principle

Directions of View

Fourier transformation of projection gives coefficients in section of "Fourier space"

Reconstruction by Fourier Synthesis Using All Sections

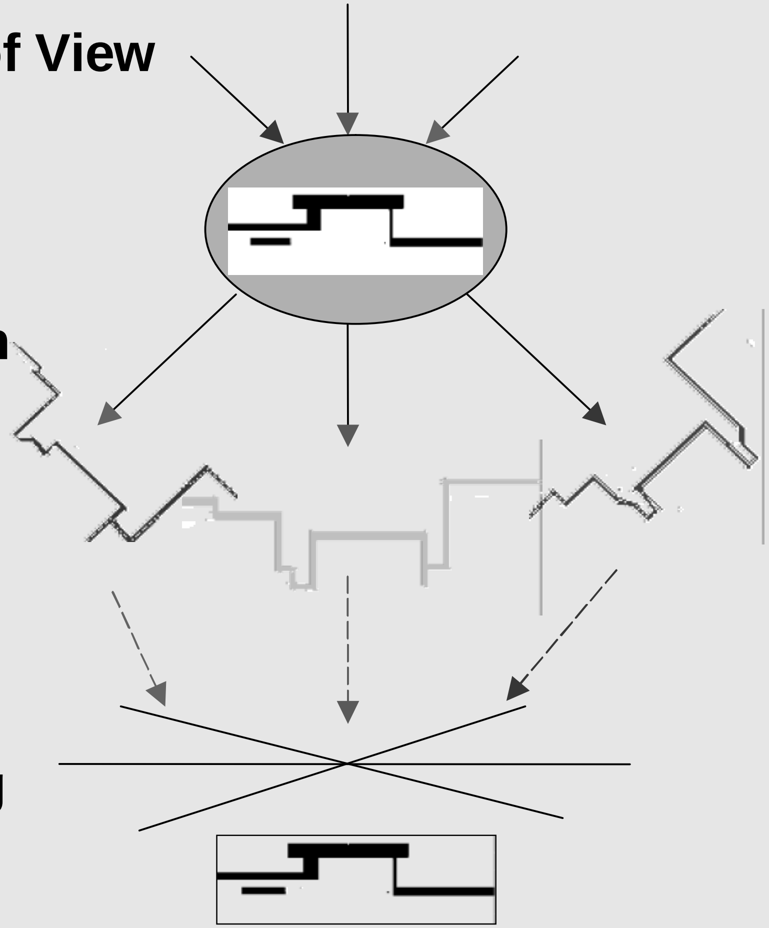

角。入射X射線透過樣品後在空間坐標系上有一個吸收投影圖P(X', θ)

$$P(x',\theta) = \ln I_0 / I = \int \mu(x,y)dy'$$

其中 I_0 和 I 分別是入射和透射X射線的強度，μ(x, y)是樣品的吸收係數，它反映了樣品在這個面上的結構信息。轉動 θ 到不同位置，可以得到一系列的投影圖。現在已經有許多方法去解出這些方程並得到吸收係數 μ (x, y)，從而就得到了這個二維圖的結構圖像。同樣由一系列二維投影圖可以求出三維的吸收係數 μ (x, x,

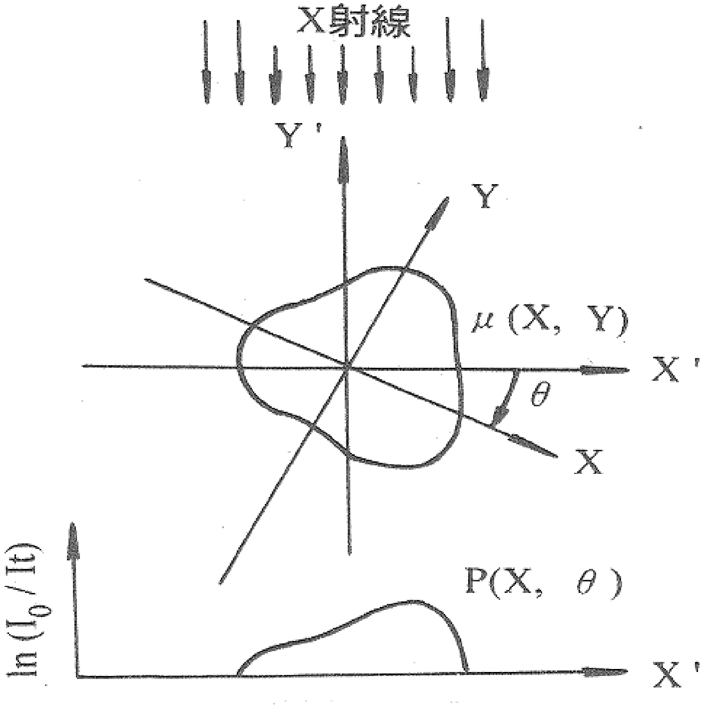

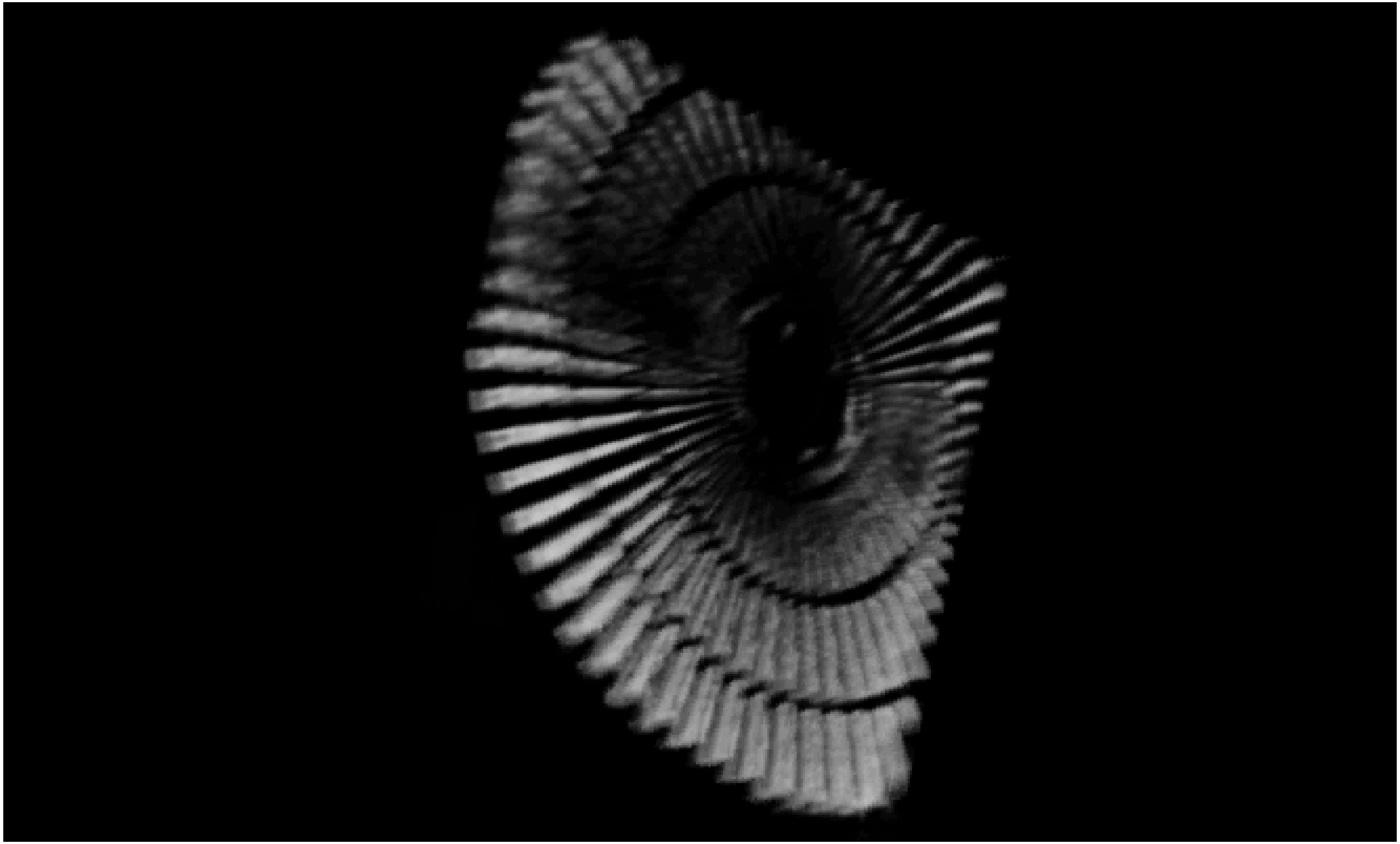

Scientific Opportunities

- Nanotechnology: 3D imaging, structure and function dependence
- Semiconductor: electromigration, failure mechanism at small dimension
- Materials and engineering: crack initiation and propagation
- Geology, agriculture, and environmental science: imaging of soil sand stones in aqueous conditions
- Biology: imaging of cells and tissues in their natural state
- Biomedical: bones, implants, dental filling, etc.

Multi-layered Cu Interconnected IC

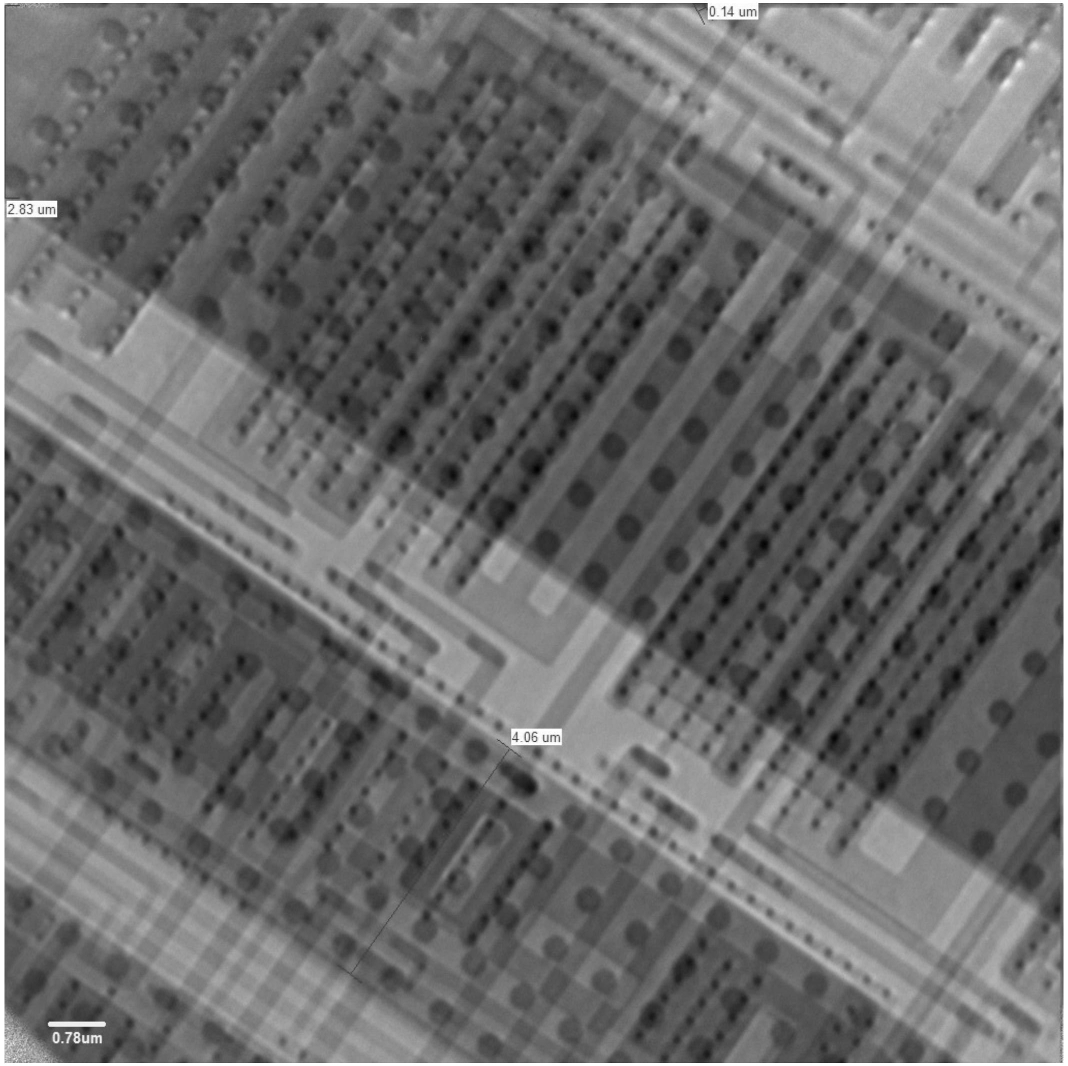

Elemental Contrast by Tuning Energy across Specific Absorption Edge

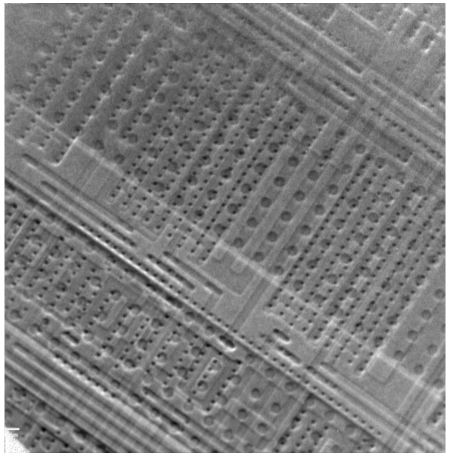

8.4 keV

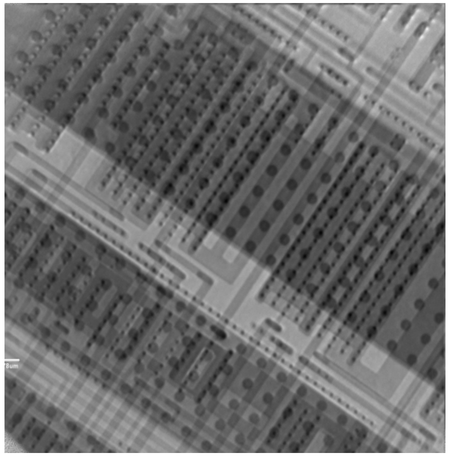

9.5 keV

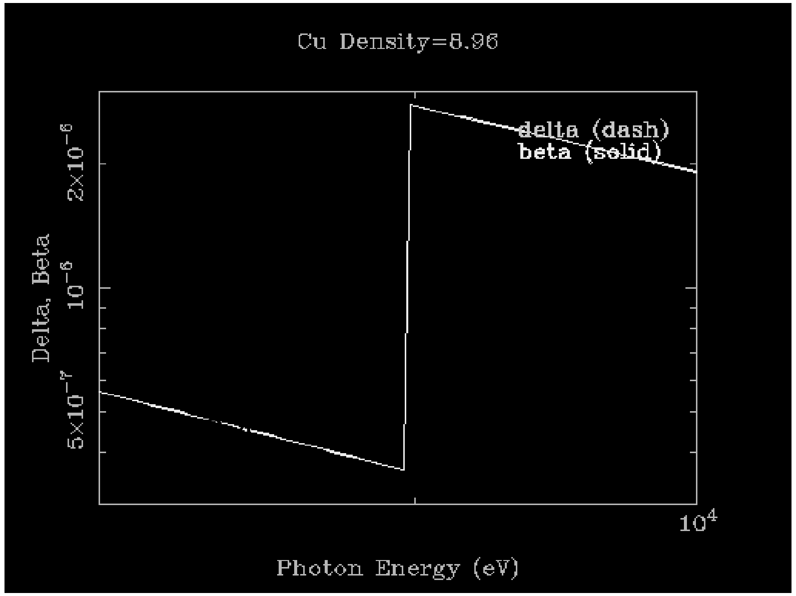

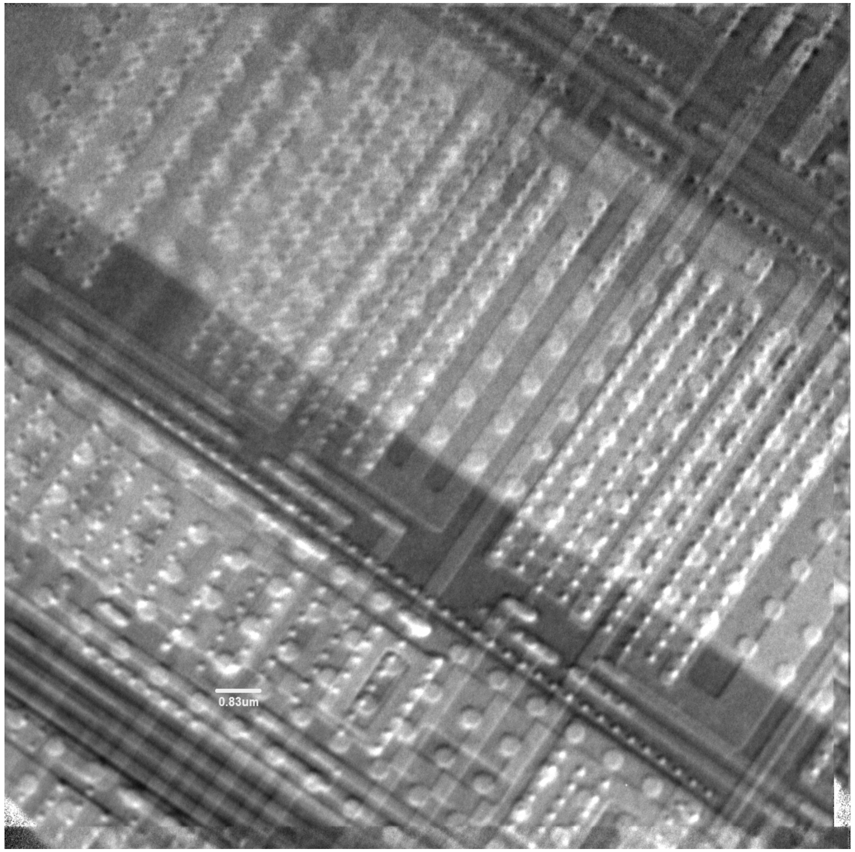

Intensity difference between
E = 8.4 keV and 9.5 keV

Investigation of Key-hole Defects in Tungsten Plugs

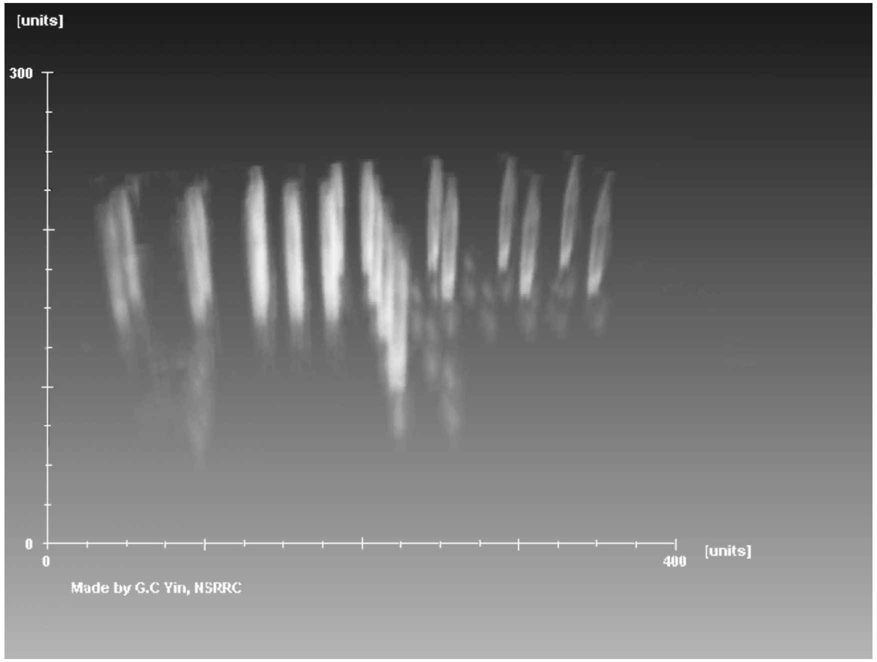

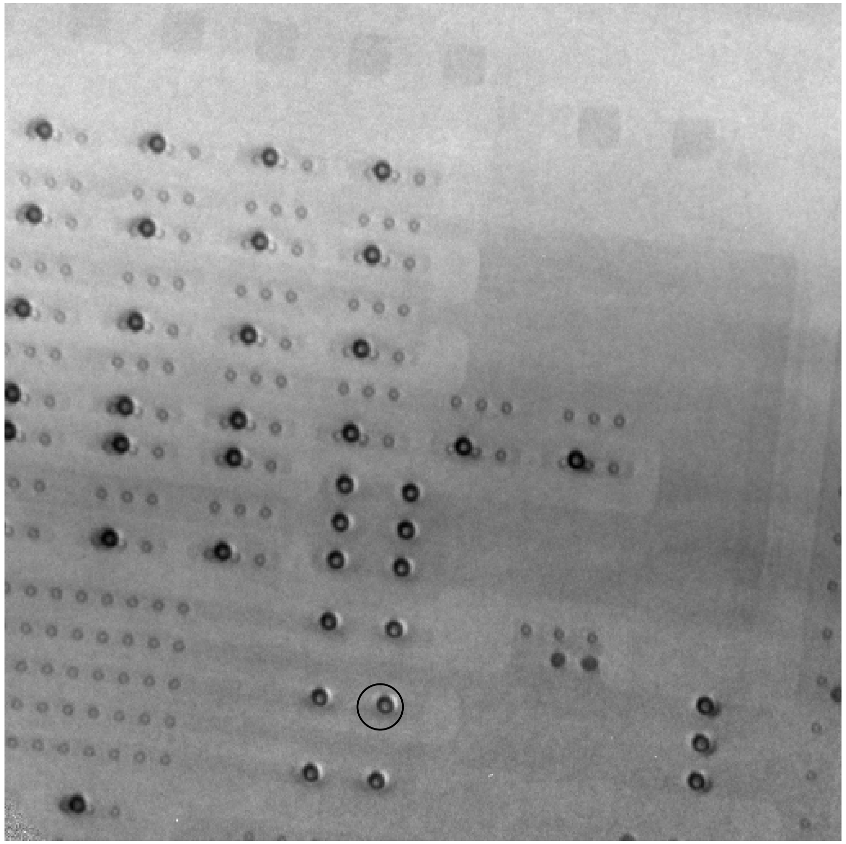

A two-dimensional projection shows the key holes

Sample provided by *Power Semiconductor Inc.*

Schematic diagram showing the process for fabricating anodic alumina film with order nanochannels

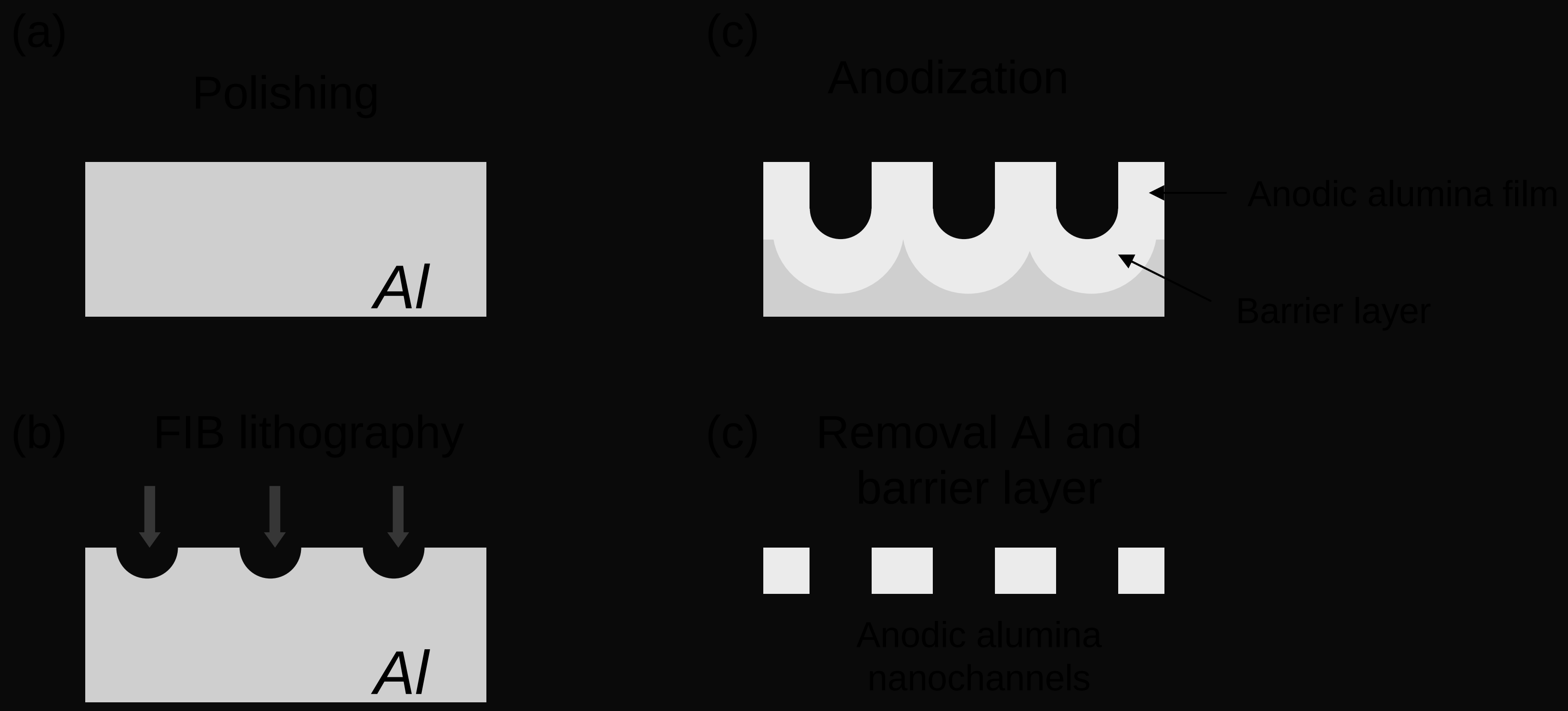

Reproduced from C Y Liu *et al*, (2001), APL, 78, 120.

Nanochannel rotation +- 5^0

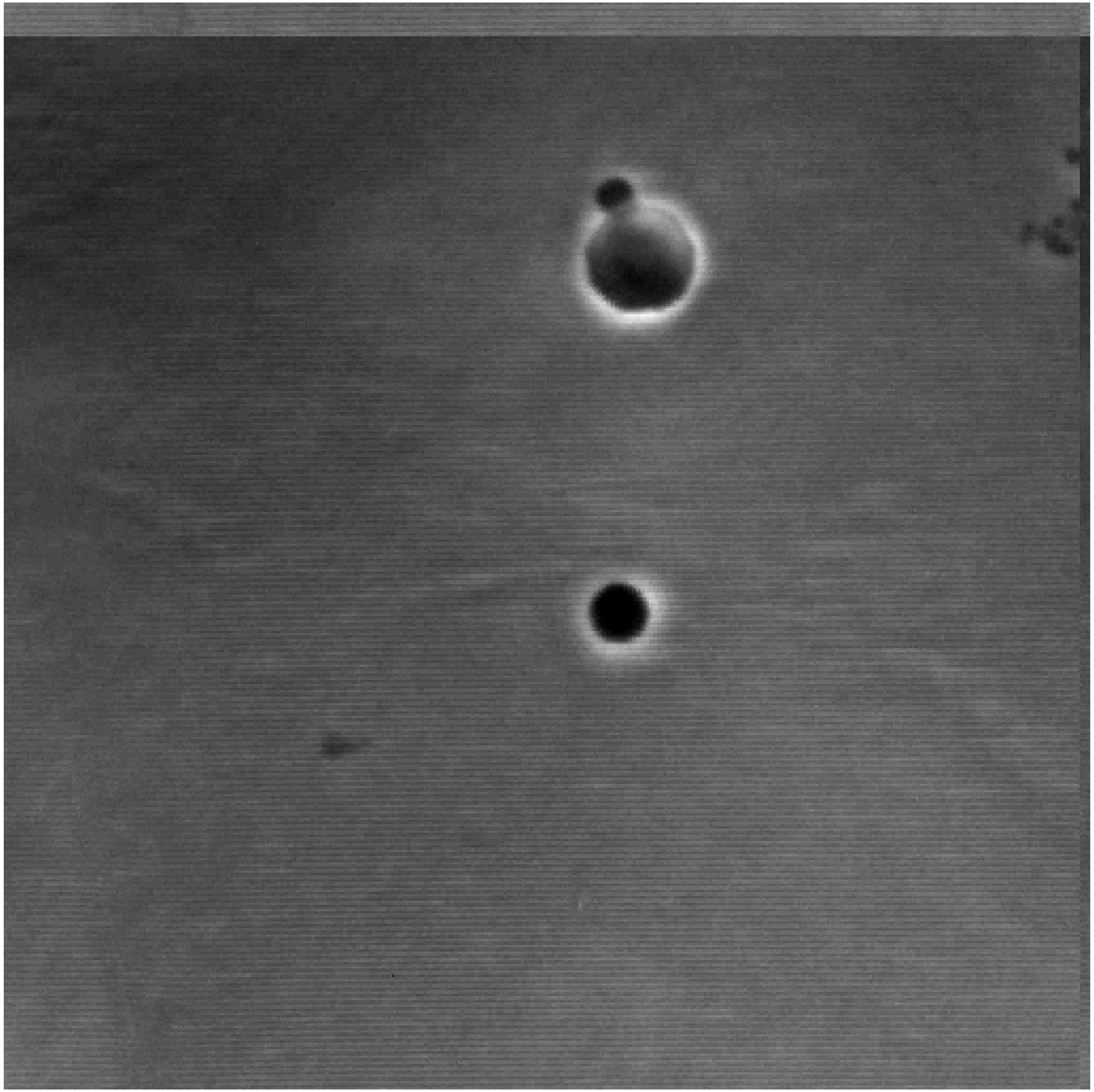

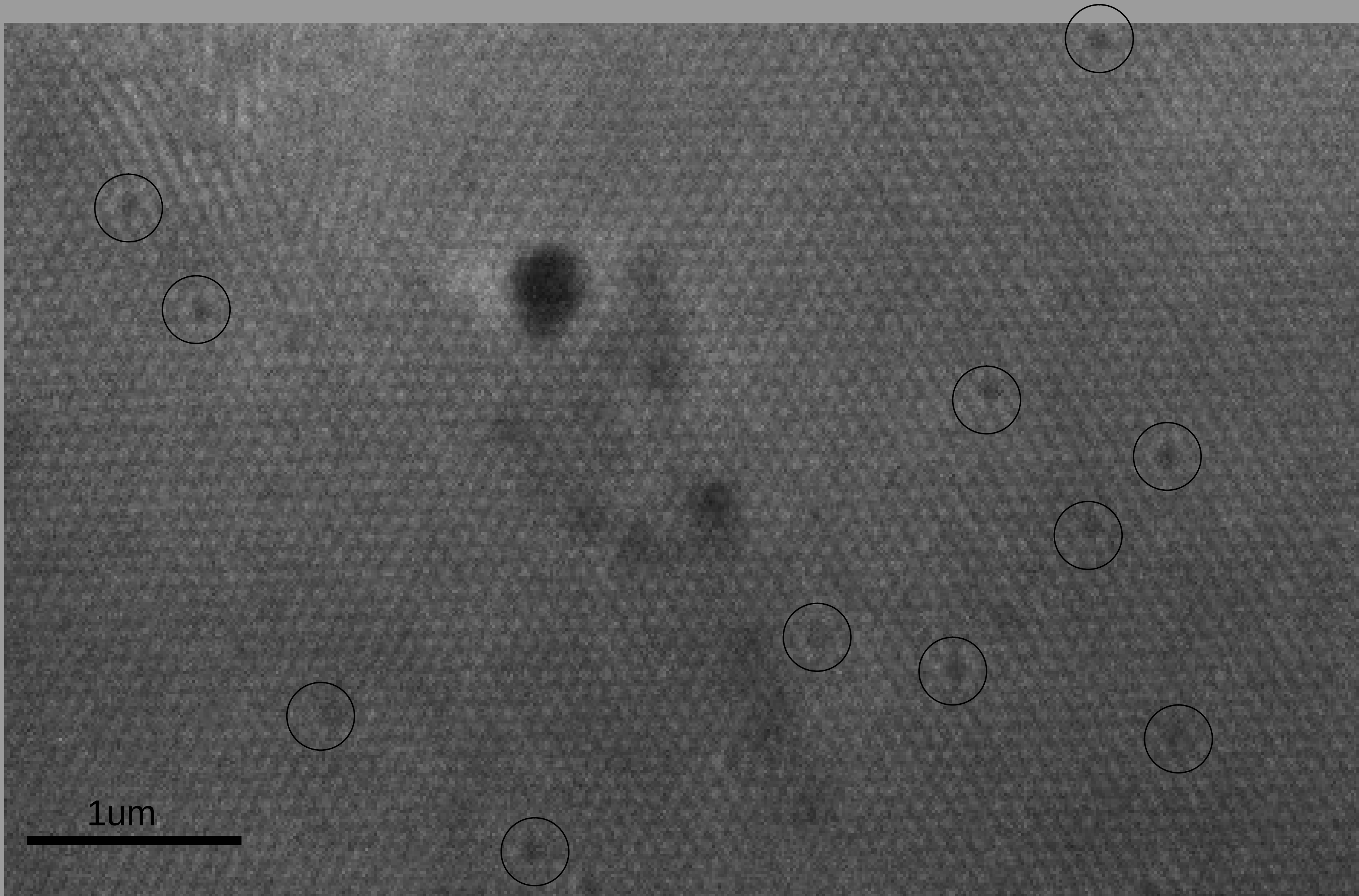
1um

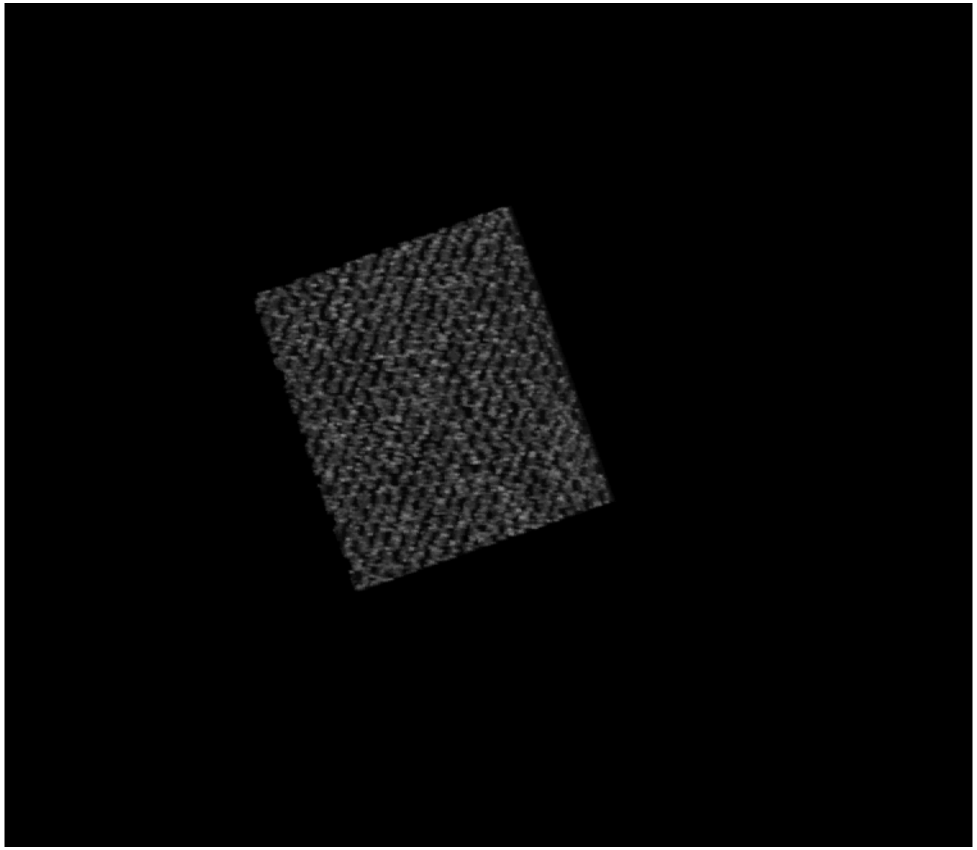

3D rendering of anodic alumina nanochannels

Virtual cross section through x-z plane.

Vimentin of the Cervix Tumor (HeLa) Cells Immuno-labelled with DAB Chromogen with Ni Enhancement

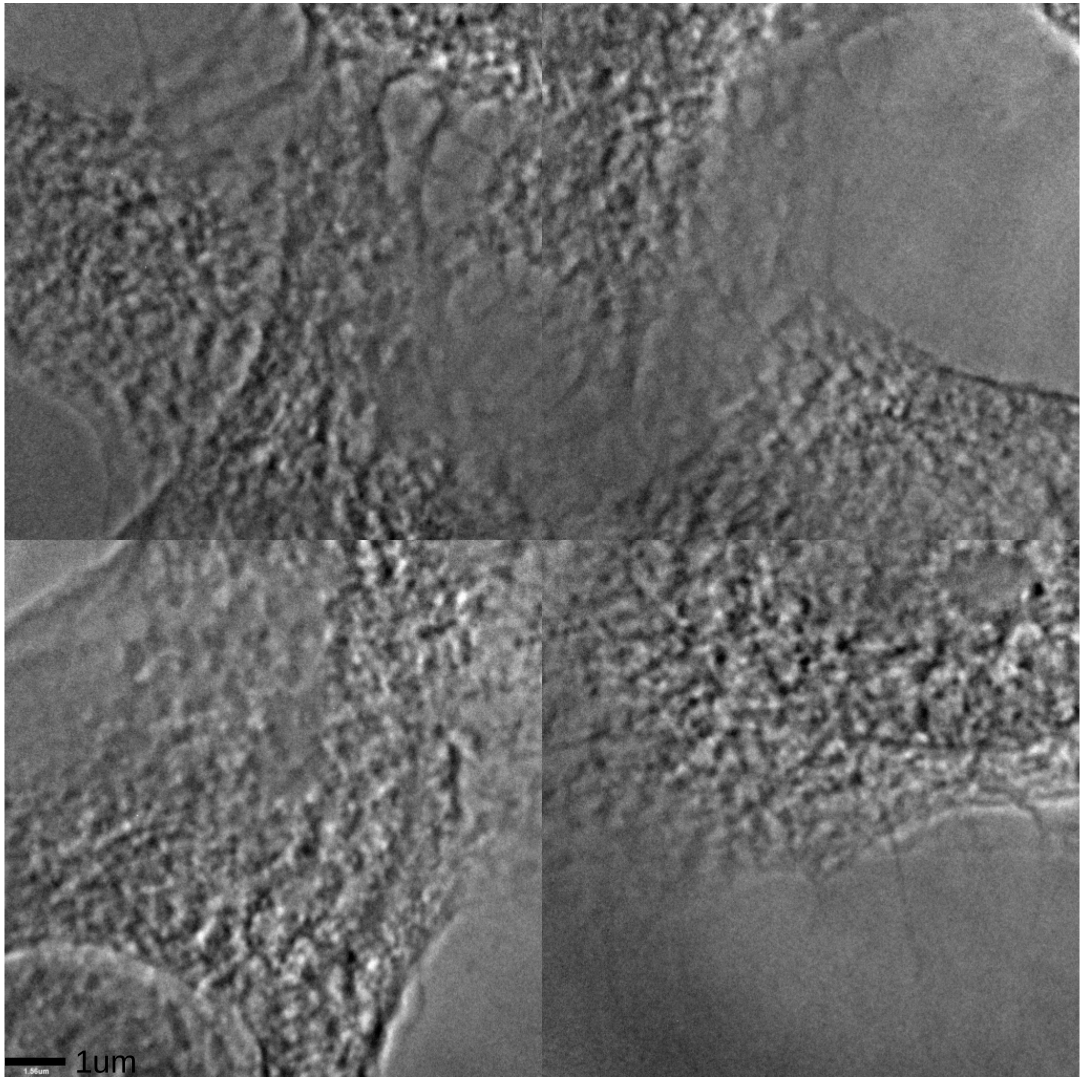

Sample provide by Yeukuang Hwu,
Academia Sinica

• Nuclear pore complex (NPC): a large (50-100 MD) collection of proteins which organize the ~9 nm openings in nuclear membranes of eukaryotic cells.

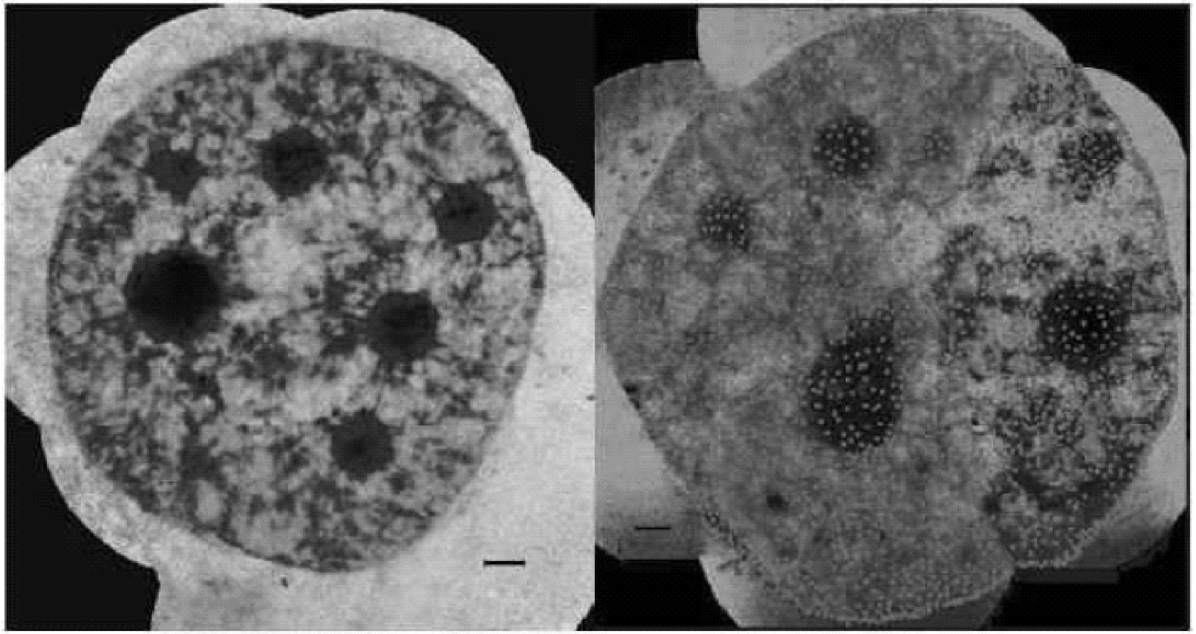

FIGURE 3. Distribution of nuclear pore complexes (NPC) in tumor mammary epithelial cells. The left image is the control, which was not exposed to primary anti-NPC antibodies but did receive secondary gold-tagged antibodies and silver enhancement, and is free of label. Blue dots in the right image are antibody labeled, silver enhanced NPC molecules. Scale bar = 1 µm.

C. Larabell (LBNL): cell biologist, using confocal & electron microscopy

• Immunocytochemistry: a method for identifying structure-function relationships of cells and proteins in cells by looking at the sub-cellular location of these proteins

• Critical proteins inside cells are labeled so that X-rays could be used to identify them

• X-ray microscopy gives cell biologists a whole new way of looking at their samples

C. Larabell (LBNL) ALS XM-1

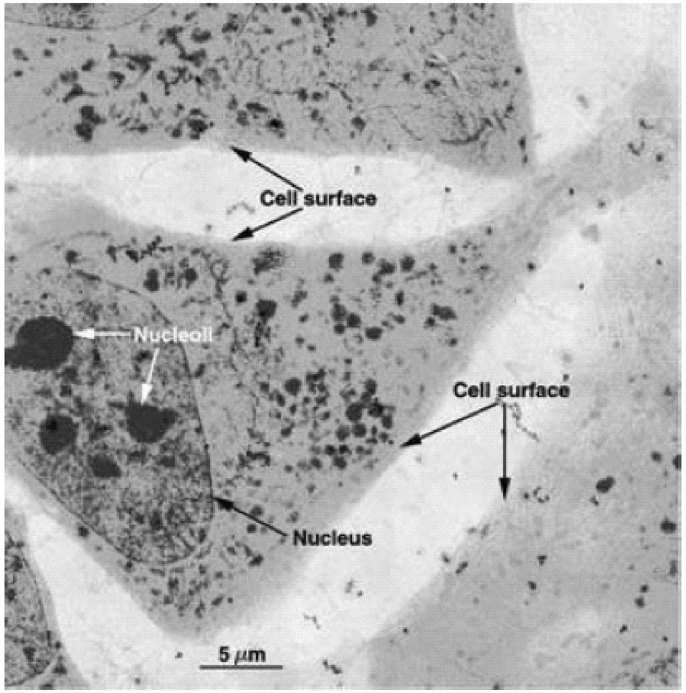

Transmission x-ray microscope image of mouse 3T3 fibroblasts, a type of connective-tissue cell, with spatial resolution of 36 nm, clearly shows features -- such as nucleoli and the sharp nuclear membrane -- not resolvable with optical confocal microscopy.

- The basic information about the organization of cells and subcellular structures is critical for our understanding of cellular functions – central theme in cell biology.

- The challenge in cell biology has been to obtain the best resolution 3D morphological information about cells that are examined in a state most closely resembling their natural environment.

- X-ray microscopy is proving to be a powerful method in that (a) it provides far better resolution thar confocal laser microscopy, and (b) one can examine whole, fully-hydrated cells, avoiding potential artifacts introduced by the dehydration, embedding and sectioning that is required for electron microscopy.

- Cellular imaging is of critical importance in the post-genomic era as we face the daunting task of determining the function of the vast number of genes and gene products identified as a result of modern molecular biology techniques.

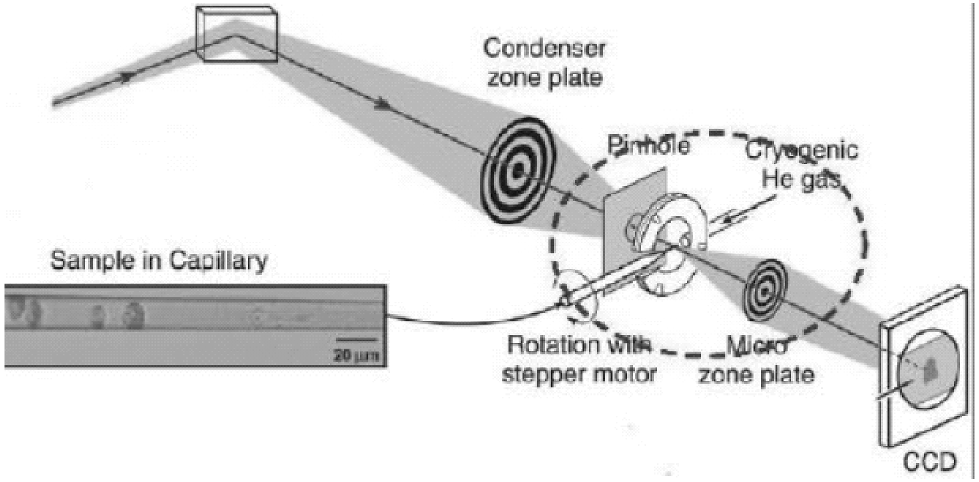

- Flash-frozen, whole, fully hydrated cells
- Soft x-ray microscope, depth of field ~10μm

=> Unique 3D information about cells and interactions of intracellular organelles

Drosophila embryonic cell
(G. Schneider, LBNL)

Green = nucleolus
Gold = sex-determining protein
(labeled with 1nm Au & Ag-enhanced)

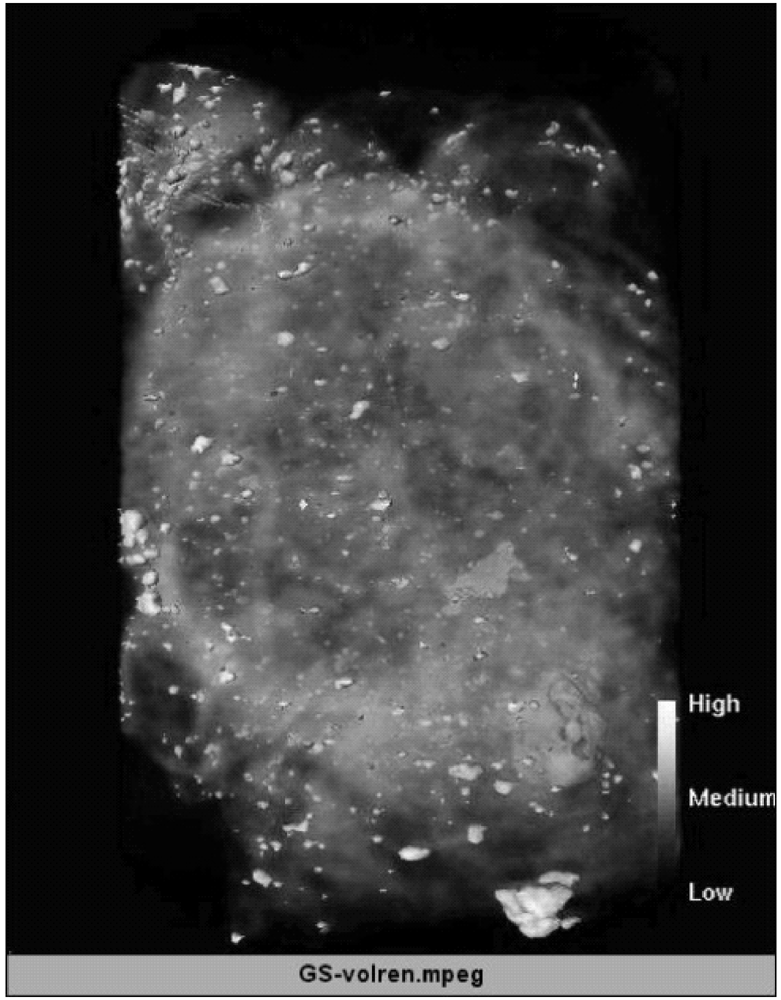

Tomography in a TXM

- TXM is *much* faster for tomography!
- D. Weiß *et al.*, *Ultramicroscopy* **84**, 185 (2000). See also G. Schneider *et al.*, *Surf. Rev. Lett.* **9**, 177 (2002)
- *Chlamydomonas reinhardtii*, frozen in liquid nitrogen.
- Rendering: organelles highlighted by optical density

衣滴蟲

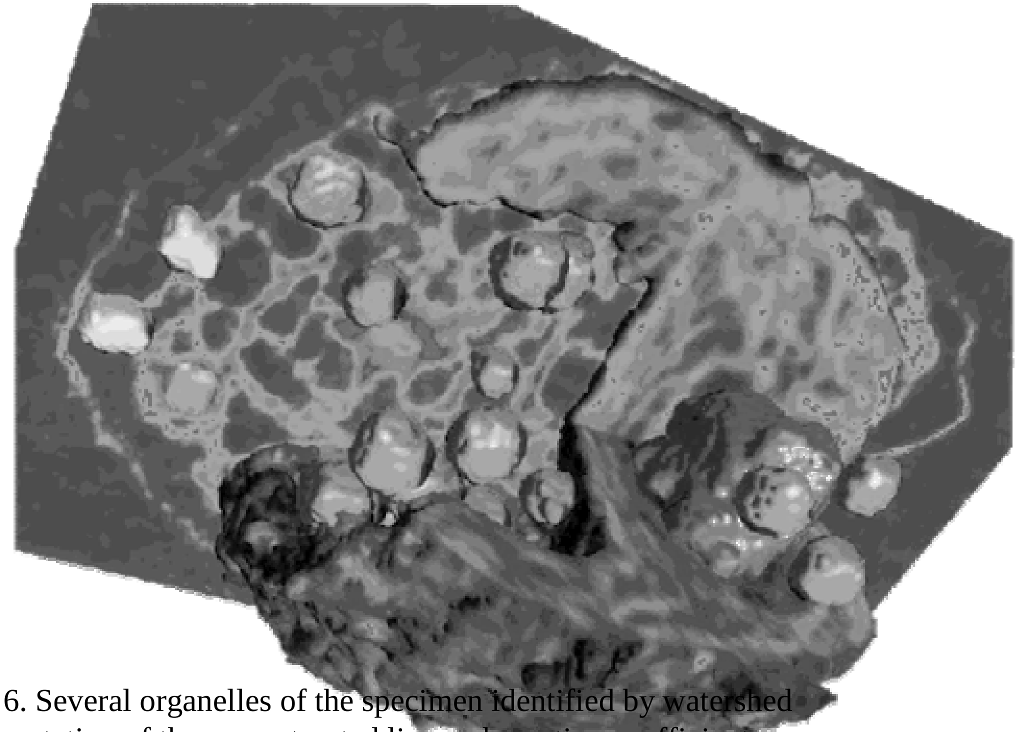

Fig. 6. Several organelles of the specimen identified by watershed segmentation of the reconstructed linear absorption coefficient (LAC): chloroplast (green), pyrenoid (blue), spherical vesicles (red), and flagellar roots (brown). One quadrant of the chloroplast has been cut away to reveal the pyrenoid. Also displayed is one slice of the reconstructed linear absorption coefficient. The diameter of the alga is approx. 7.4 mm. Visualization using the Amira system developed at ZIB (http://amira.zib.de).

Chromosome Immuno-labelled by Au nano-particles

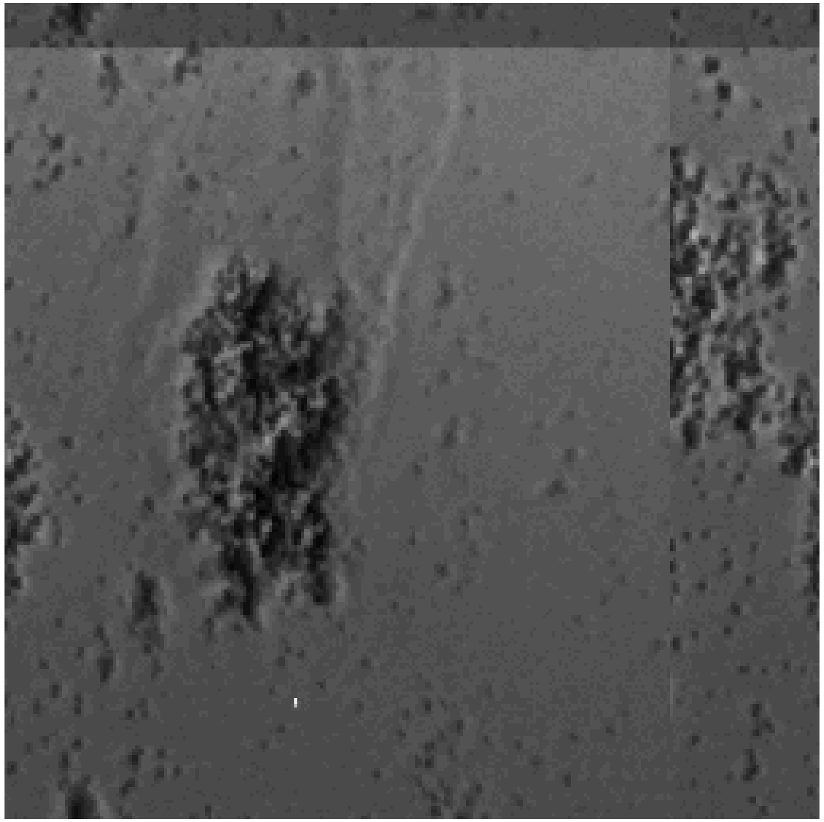

Incoperated with C-H Lin of NYMU

Wing Scale of Papilio Bianor

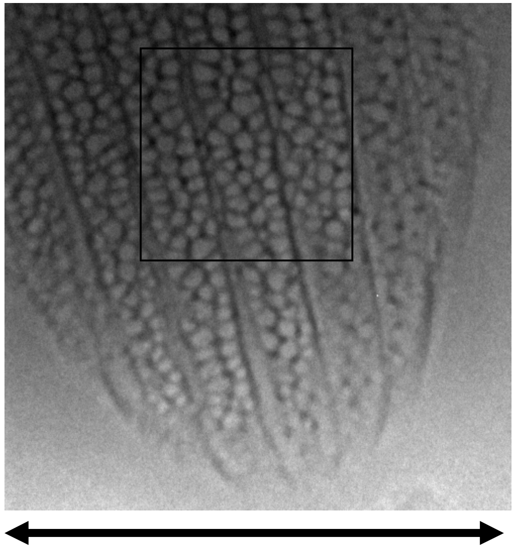

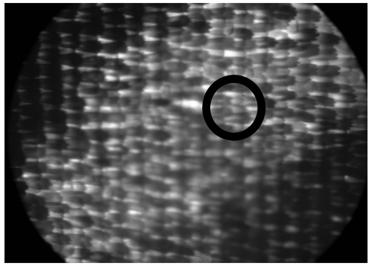

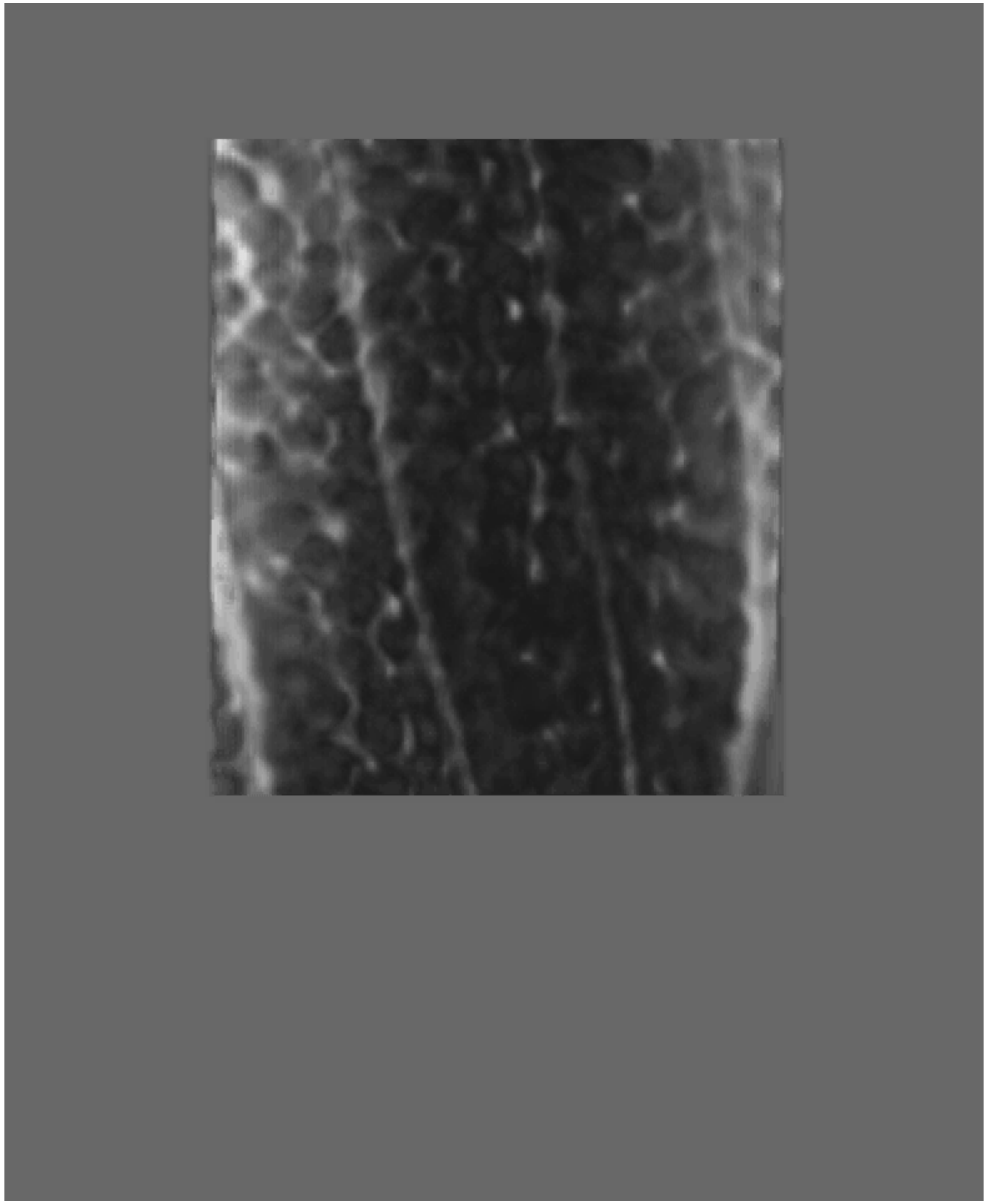

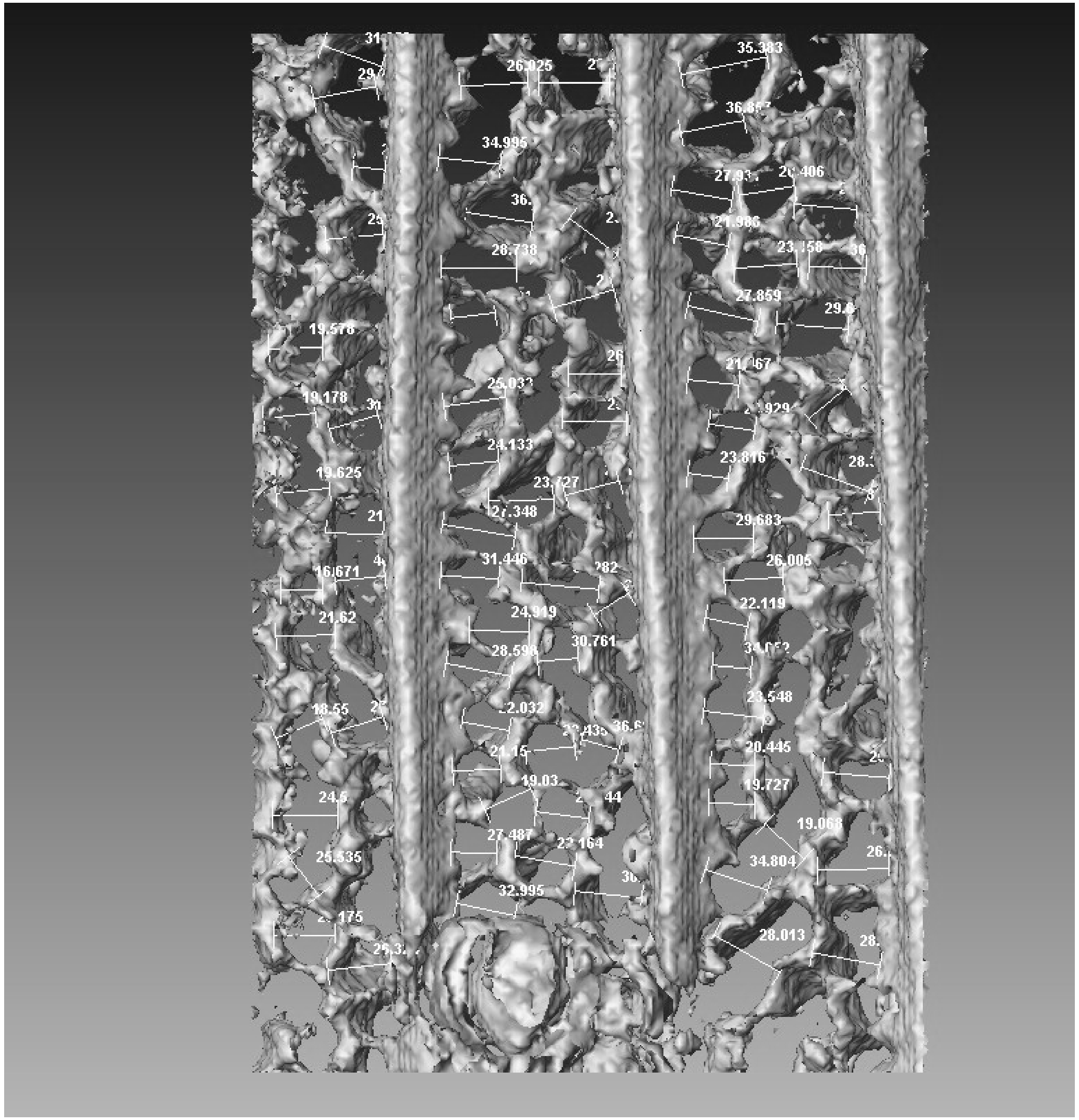

35.383
26.025
34.995
21.986
28.738
27.859
19.578
25.032
19.178
24.133
23.816
19.625
23.727
29.683
31.446
26.005
24.919
22.119
21.62
30.761
28.598
23.548
18.55
20.445
19.727
19.068
27.487
23.164
34.804
25.535
32.995
28.013

孔雀青蛺蝶

SEM

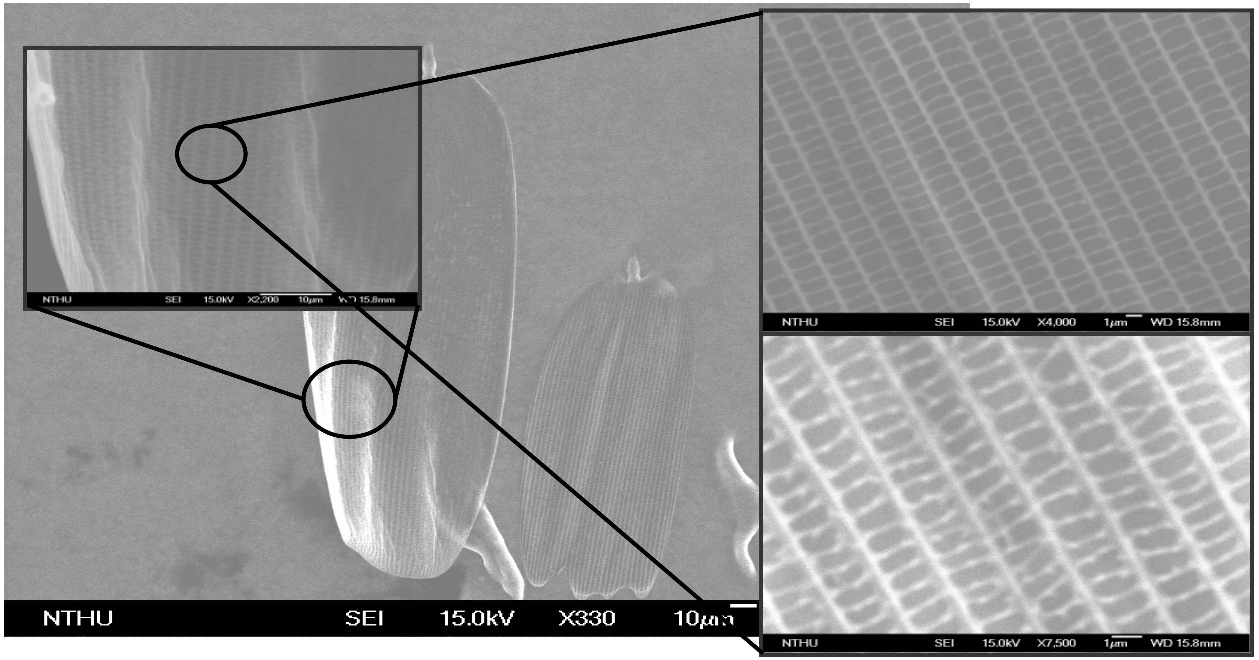

TXM with phase contrast

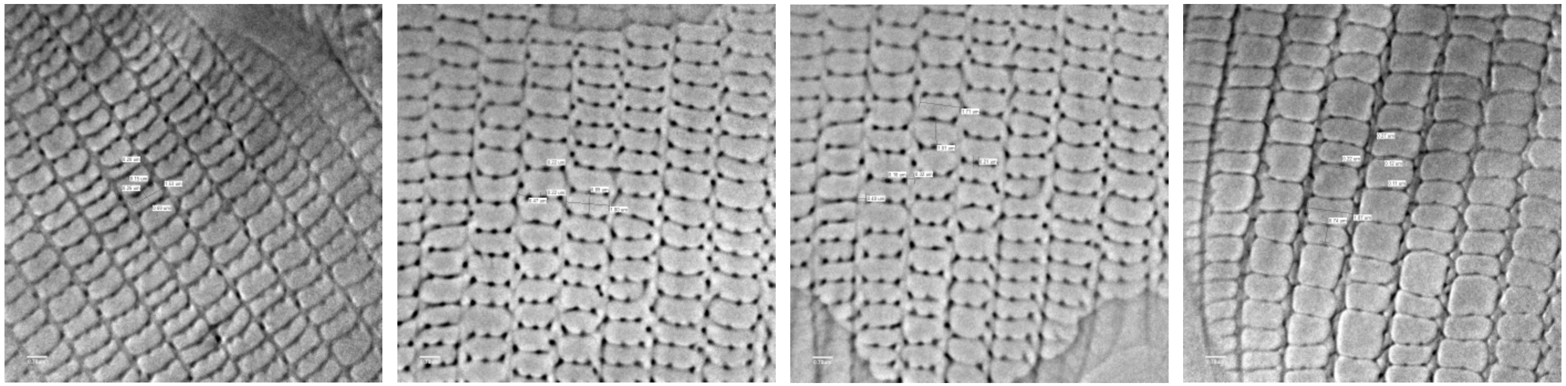

Bacteria Mediated Stainless Steel Corrosion

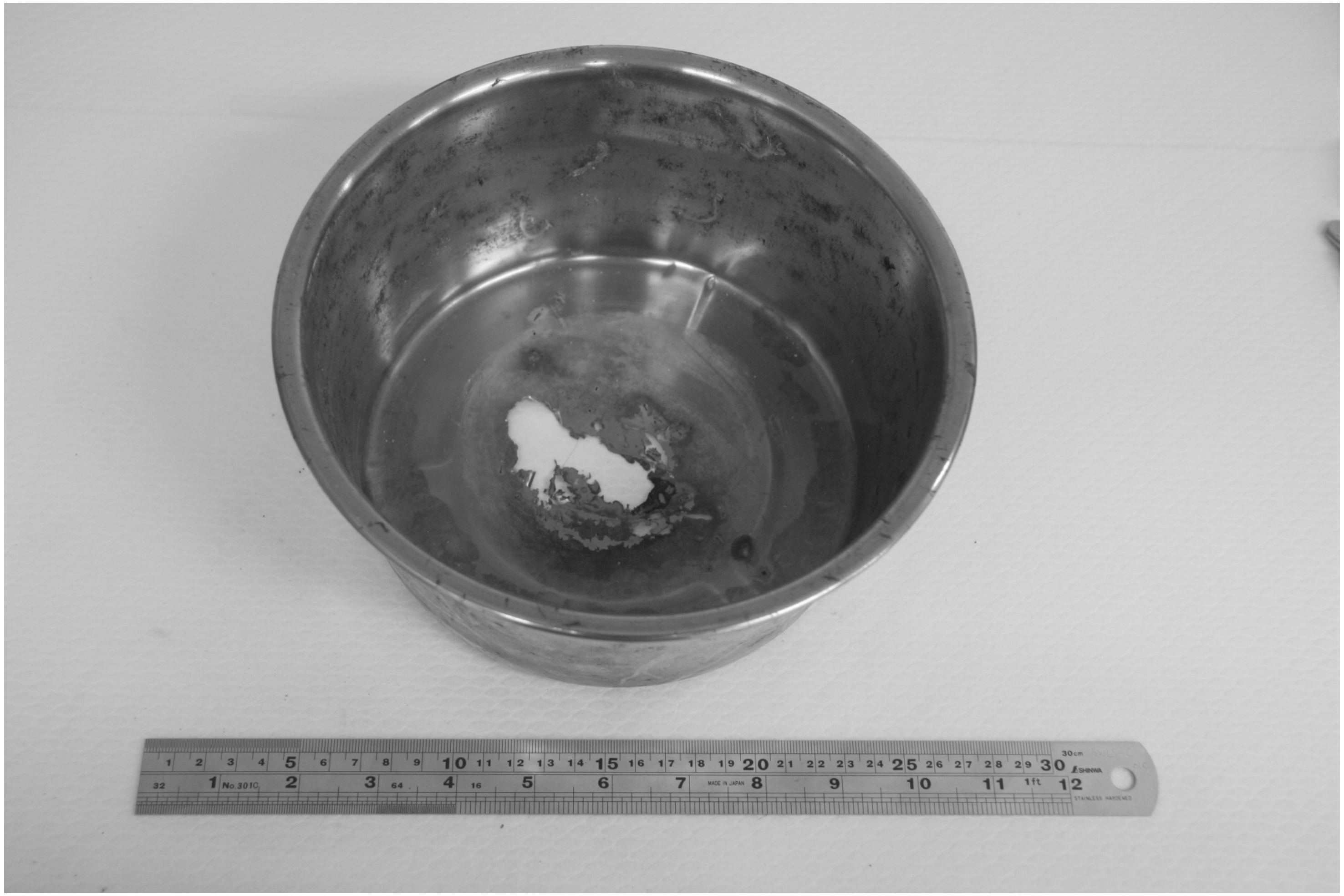

Incoperated with C-S Jean of NCKU

Bacteria Mediated Stainless Steel Corrosion

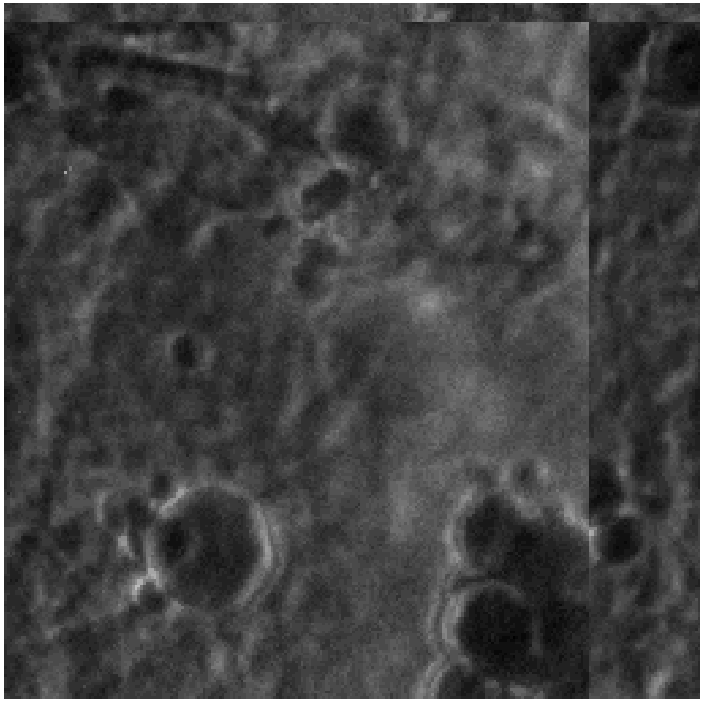

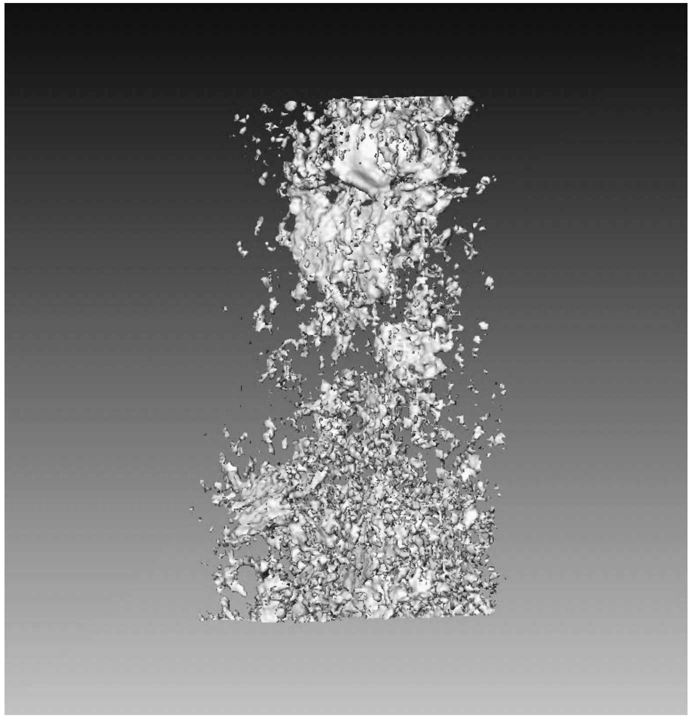

Incooperated with C-S Jean of NCKU

Taiwan Chelungpu-fault Drilling Project (TCDP)

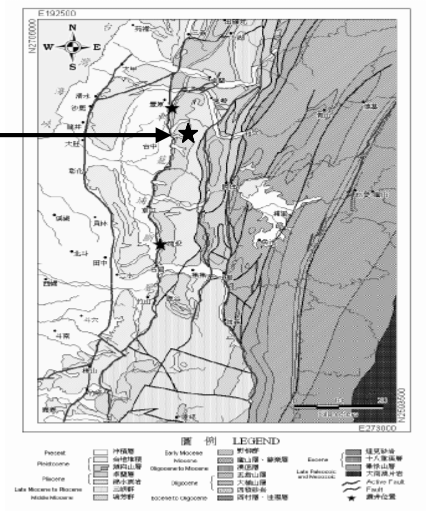

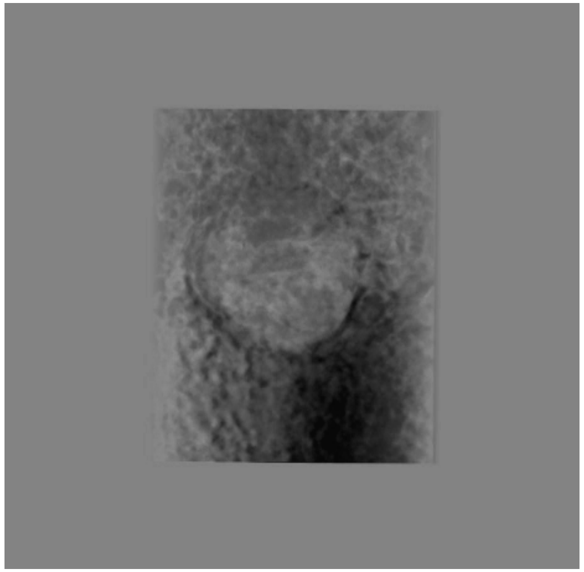

TXM 1111.29m (phase contrast)

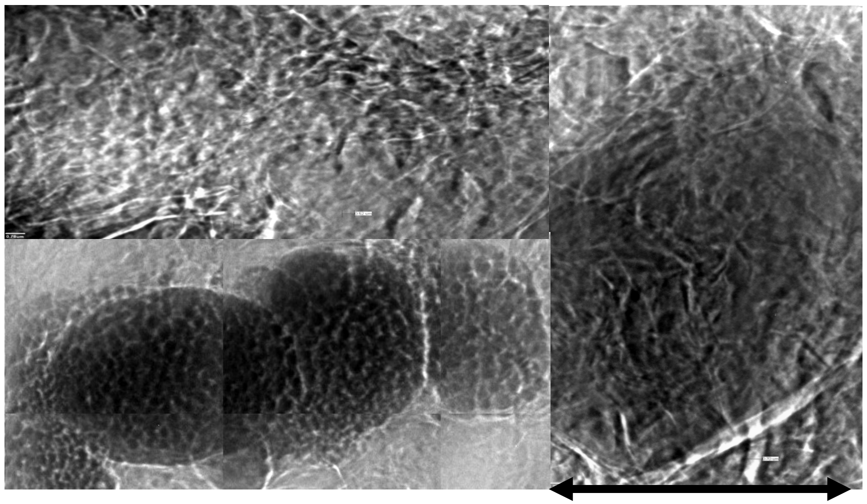

15um

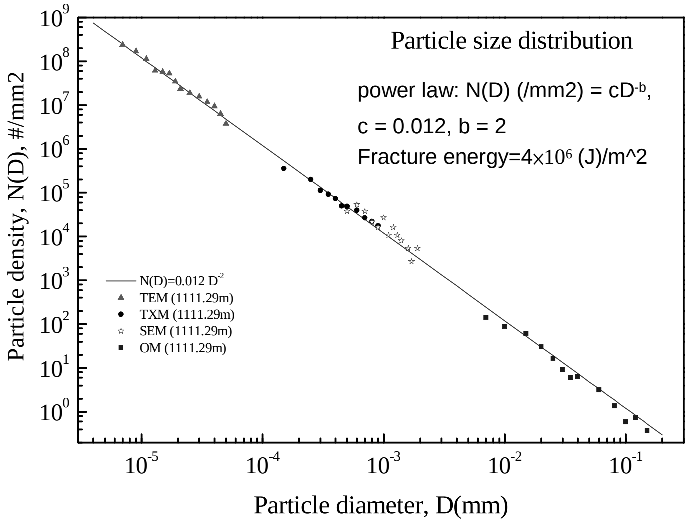

Alignment of Image Series

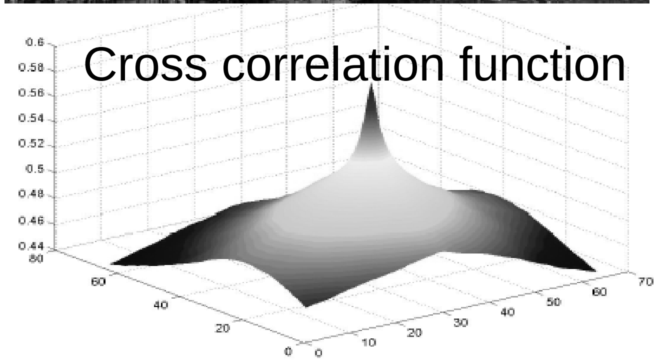

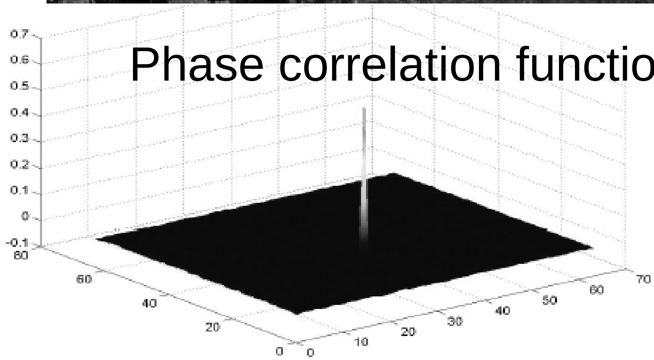

$C(x,y) = FT^{-1}\{FT(I_1)FT(I_2)^*\}$

$P(x,y) = FT^{-1}\{FT(I_1)FT(I_2)^* / |FT(I_1)FT(I_2)^*|\}$

Incorporated with Fu-Rong Chen, *National Tsing-Hua University*

Before alignment

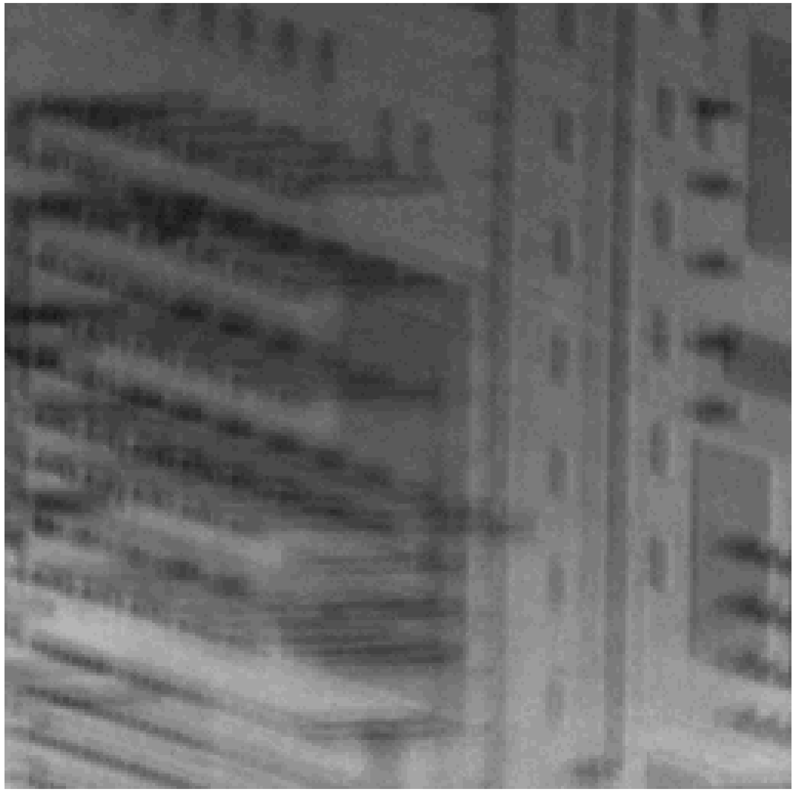

Aligned by phase correlation function

TIE(Transport Intensity Equation)
(Non-interference Phase Retrieval)

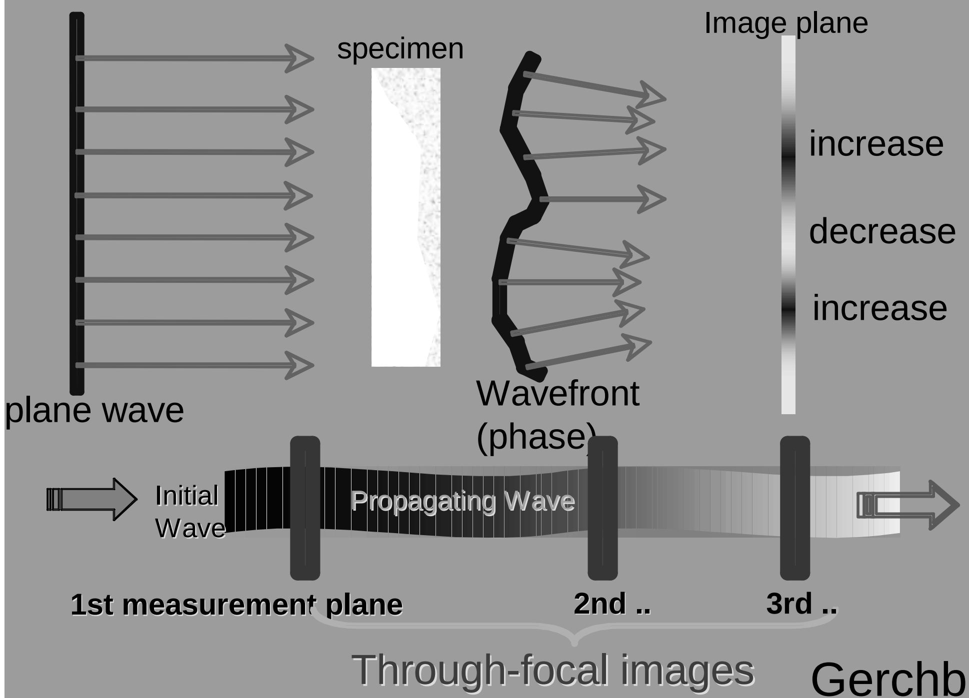

$$\nabla_{\perp}\bullet(I(r_{\perp},0)\ \nabla_{\perp}\varphi)=-k\partial_{z}I(r_{\perp},z)$$

in-focus image — Two de-focus images

Gerchberg-Saxton Algorithm

Incorporated with Fu-Rong Chen, *National Tsing-Hua University*

Phase Retrieval of Fault Rocks

17 images

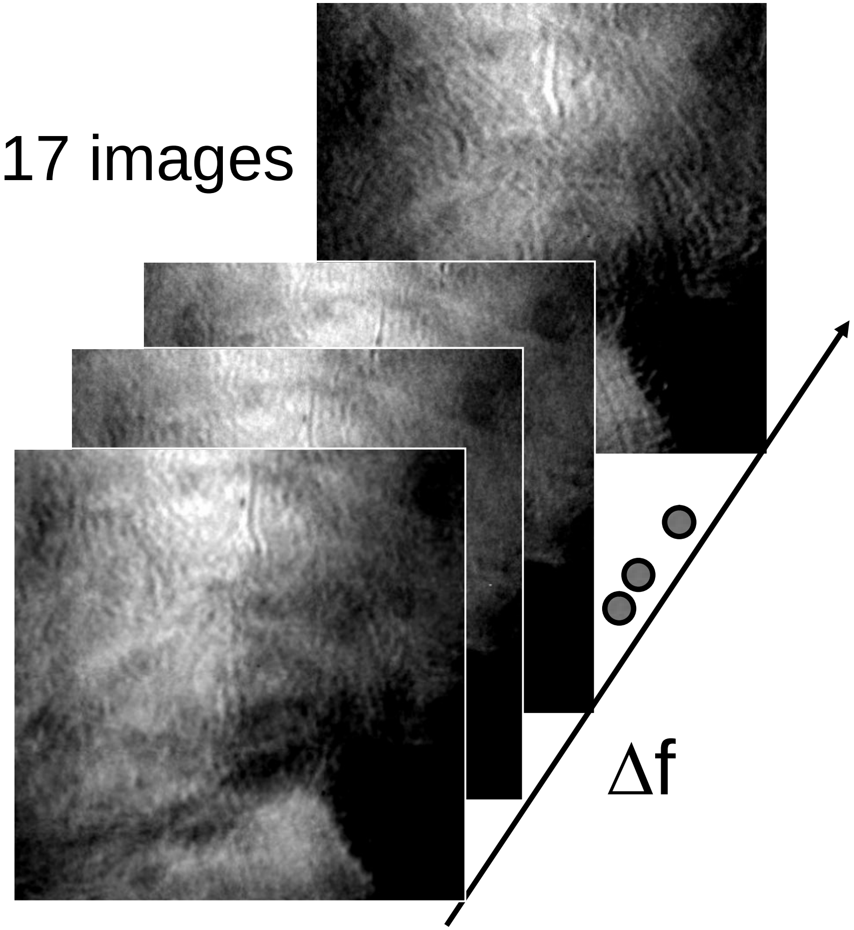

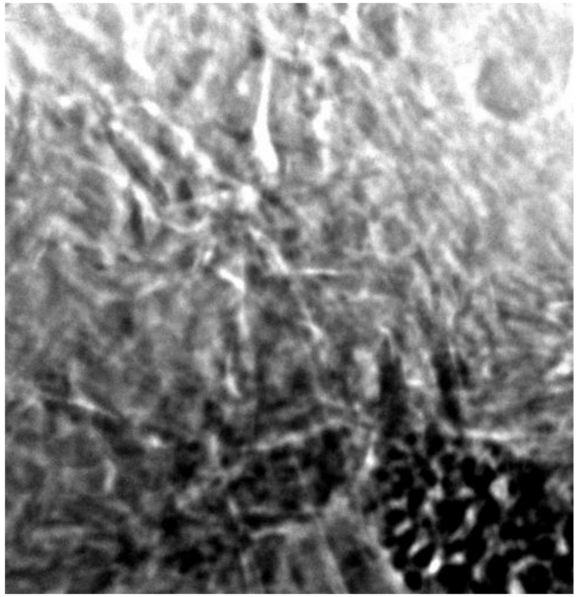

Phase image from Zernike Phase Ring

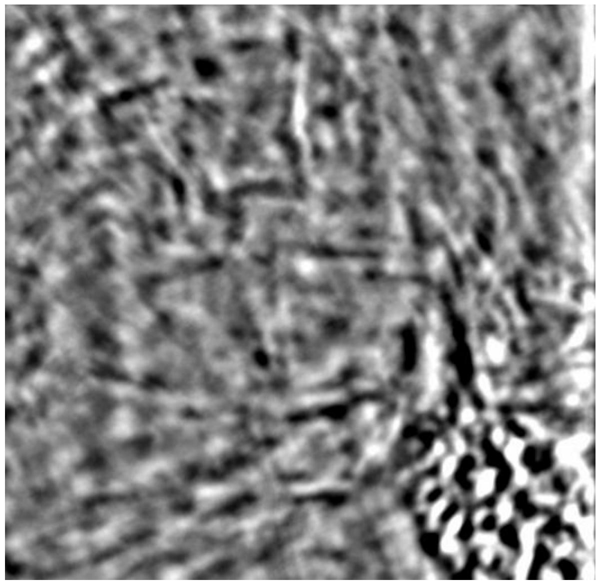

Reconstructed Phase

Performance of NSRRC TXM

Energy 8-11 keV	Spatial resolution (nm)	Phase contrast	2D Field Of View (μm)	3D Tomography volume (μm)
2D	60	Yes	15x15	-
	30	(Yes, 2005)	5x5	-
3D	60x60x60	Yes	-	15x15x15
	(30x30x30)	(Yes, 2005)	-	(5x5x5)
Material analysis capability	Cu, Zn, Ga, Ge, As, Ta, W, Au, Hg, Pb, etc.			

Performance of world wide Full Field X-ray Microscopy

	NSRRC (Taiwan)	ESRF (Europe)	ALS (U.S.)	Spring-8 (Japan)
Type	Full-Field Hard X-ray	Full-Field Hard X-ray	Full-Field Soft X-ray	Full-Field Hard X-ray
Energy	8-11Kev variable	4Kev Fixed	270~500ev Water window	8.75 Kev Fixed
Resolution	30nm 60nm Phase contrast	60nm Phase contrast	15nm	250nm
Penetration depth	Above 100um Silicon	Below 10um silicon	1~2um for soft material	Above 100um Silicon
DOF	50um	10~20 um	1~0.5 um	200um

Fast Freeze Cryo Fixation Strongly Mitigates Radiation Dose Effects

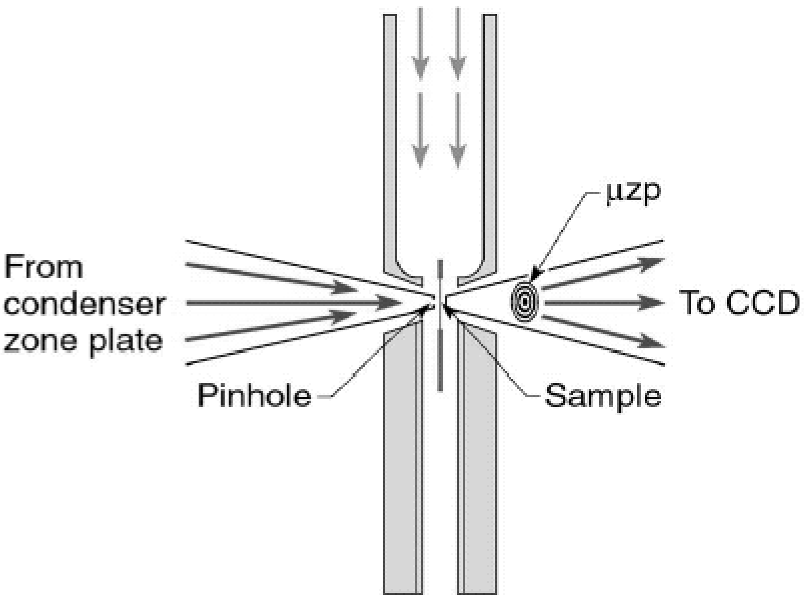

- Holds wet sample sandwiched between two Silicon Nitride windows
- Helium passes through LN, is cooled, and directed onto sample windows

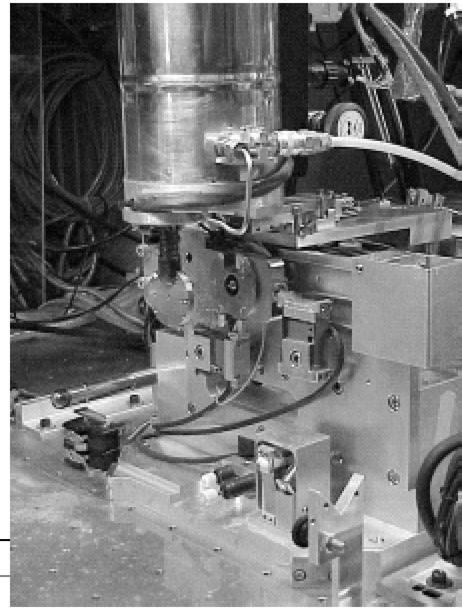

Fast Freeze

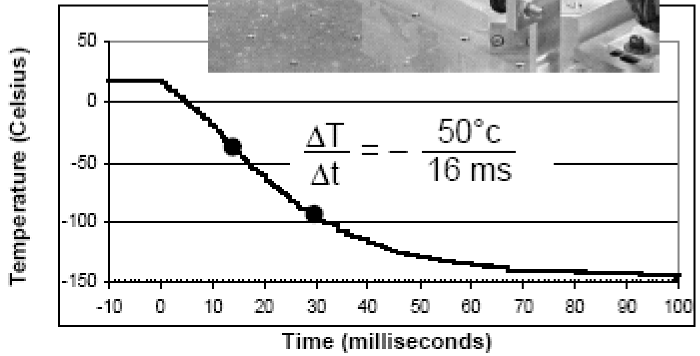

W. Meyer-Ilse, G. Denbeaux, L. Johnson, A. Pearson / CXRO-LBNL

Fast Freeze Cryo Fixation Strongly Mitigates Radiation Dose Effects

Cryogenically Fixed 3T3 Fibroblast Cells

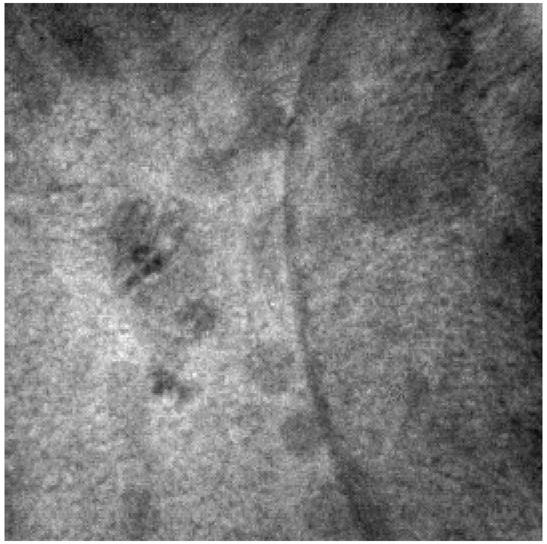

1st Exposure

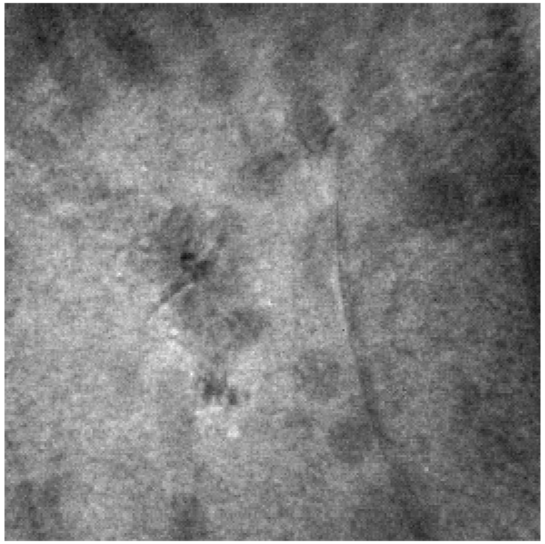

40th Exposure

W. Meyer-Ilse, W. Bates, G. Denbeaux, L. Johnson, A. Pearson / MSD
C. Larabell, D. Yager, T. Shin / Life Sciences Division

Conclusions

1. The NSRRC nano-TXM has demonstrated the 2D and 3D imaging capabilities with sub-60 nm spatial resolution.
2. Sub-30nm spatial resolution is achieved by using 3rd diffraction of zone plate.
3. The capability of phase contrast has been demonstrated.
4. Future developments include the cryomicroscopy, elemental contrast, sample preparation, optical upgrade, etc.

Acknowledgements

National Synchrotron Radiation Research Center

Yen-Fang Song, Guan-Chian Yin, Jian-Hua Chen and Keng S. Liang

National Tsing-Hua University

Fu-Rong Chen, I-Ming Chen

National Yangming University

Chih-Hung Lin

National Taiwan University

Shen-rong Song, Pei-Lin Wang

National Taiwan University of Science and Technology

Bing-Joe Hwang

National Cheng-Kung University

J-S Jean

Yuan-Ze University

Tseng-Hao Ko

Academia Sinica

Yeukuang Hwu, Yu-Lin wang, Typhoon Lee

Xradia Inc.

Fred Duewer, Wenbing Yun

Thank you for your attention.